A TRIDENT SCHOLAR
PROJECT REPORT

NO. 249

REACTION KINETICS OF
Sc, V, Cr, Co AND Ni WITH N_2O

UNITED STATES NAVAL ACADEMY
ANNAPOLIS, MARYLAND

20031201 117

REPORT DOCUMENTATION PAGE

Form Approved
OMB No. 074-0188

1. AGENCY USE ONLY (Leave blank)	2. REPORT DATE 7 May 1997	3. REPORT TYPE AND DATE COVERED

4. TITLE AND SUBTITLE
Reaction kinetics of Sc, V, Cr, Co and Ni with N_2O

5. FUNDING NUMBERS

6. AUTHOR(S)
Erica J. Kölsch

7. PERFORMING ORGANIZATION NAME(S) AND ADDRESS(ES)

U.S. Naval Academy
Annapolis, MD

8. PERFORMING ORGANIZATION REPORT NUMBER

USNA Trident Scholar project report
no. 249 (1997)

9. SPONSORING/MONITORING AGENCY NAME(S) AND ADDRESS(ES)

10. SPONSORING/MONITORING AGENCY REPORT NUMBER

11. SUPPLEMENTARY NOTES
Accepted by the U.S. Trident Scholar Committee

12a. DISTRIBUTION/AVAILABILITY STATEMENT
This document has been approved for public release; its distribution is UNLIMITED.

12b. DISTRIBUTION CODE

13. ABSTRACT: The purpose of this experiment was to determine the gas phase reactivities of N_2O with the following first-row transition metal atoms: $Sc(a^2D_{3/2})$, $V(a^4F_{3/2})$, $Cr(a^7S_3)$, $Co(a^4F_{9/2})$ and $Ni(a^3D_3, a^3F_4)$. Reactions were studied in the temperature range of 298K-623K. Sc, V, Cr, Co and Ni atoms were produced by photodissociatioon of $Sc(hfa)_3$, $Sc(TMHD)_3$, $V(CO)_6$, $V(CO)_4(C_5H_5)$, $V(C_5H_5)_2$, $Cr(CO)_6$, $Co(C_5H_5)(CO)_2$ and $Ni(C_5H_5)_2$ respectively. Pseudo first-order conditions were maintained ([Transition Metal]$<<$[N_2O]), and atoms were detected using a laser-induced flourescence technique. Reactions of the ground states with N_2O were temperature dependent. Reactions of Sc, V, Cr and Co with N_2O were found to be pressure independent, indicating a bimolecular abstraction mechanism. Removal rate constants for the excited a^5D_J and a^5S_2 states of Cr were found to be fast compared to reactions with the ground state. The rate constants for Sc, V, Cr and Co can be described in Arrhenius form ($k=A\exp(-E_a/RT)$) by $k=1.6\times10^{-10}\exp(-11.7 \text{ kJ/mol}/RT)$ cm^3s^{-1}, $k=4.6\times10^{-11}\exp(-10.7 \text{ kJ/mol}/RT)$ cm^3s^{-1}, $k=4.2\times10^{-11}\exp(-20.4 \text{ kJ/mol}/RT)$ cm^3s^{-1}, and $k=2.0\times10^{-10}\exp(-49.1 \text{ kJ/mol}/RT)$ cm^3s^{-1}, respectively. The rate constants for Ni were found to be pressure dependent at low temperatures suggesting a termolecular reaction.

q14. SUBJECT TERMS
reaction kinetics, activation energy, resonance interaction correlations

15. NUMBER OF PAGES

16. PRICE CODE

17. SECURITY CLASSIFICATION OF REPORT	18. SECURITY CLASSIFICATION OF THIS PAGE	19. SECURITY CLASSIFICATION OF ABSTRACT	20. LIMITATION OF ABSTRACT

U.S.N.A. --- Trident Scholar project report; no. 249 (1997)

REACTION KINETICS OF
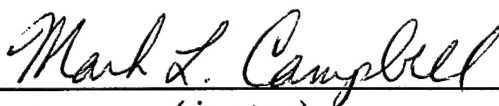## Sc, V, Cr, Co AND Ni WITH N_2O

by

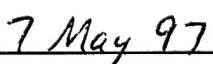Midshipman Erica J. Kölsch, Class of 1997
United States Naval Academy
Annapolis, Maryland

_____
(signature)

Certification of Advisor Approval

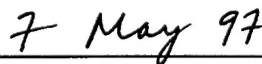Associate Professor Mark L. Campbell
Department of Chemistry

_____
(signature)

_____
7 May 97
(date)

Acceptance for the Trident Scholar Committee

Professor Joyce E. Shade
Chair, Trident Scholar Committee

_____
(signature)

_____
7 May 97
(date)

USNA-1531-2

ABSTRACT

The purpose of this experiment was to determine the gas phase reactivities of N_2O with the following first-row transition metal atoms: $Sc(a^2D_{3/2})$, $V(a^4F_{3/2})$, $Cr(a^7S_3)$, $Co(a^4F_{9/2})$ and $Ni(a^3D_3, a^3F_4)$. Reactions were studied in the temperature range of 298K - 623K. Sc, V, Cr, Co and Ni atoms were produced by photodissociation of $Sc(hfa)_3$, $Sc(TMHD)_3$, $V(CO)_6$, $V(CO)_4(C_5H_5)$, $V(C_5H_5)_2$, $Cr(CO)_6$, $Co(C_5H_5)(CO)_2$ and $Ni(C_5H_5)_2$, respectively. Pseudo first-order conditions were maintained ([Transition Metal] $<<$[N_2O]), and atoms were detected using a laser-induced fluorescence technique. Reactions of the ground states with N_2O were temperature dependent. Reactions of Sc, V, Cr and Co with N_2O were found to be pressure independent, indicating a bimolecular abstraction mechanism. Removal rate constants for the excited a^5D_J and a^5S_2 states of Cr were found to be fast compared to reactions with the ground state. The rate constants for Sc, V, Cr and Co can be described in Arrhenius form ($k= Aexp(-E_a/RT)$) by $k=1.6\times10^{-10}exp(-11.7 \text{ kJ/mol}/RT)$ cm^3s^{-1}, $k= 4.6\times10^{-11}exp(-10.7 \text{ kJ/mol}/RT)$ cm^3s^{-1}, $k=4.2\times10^{-11}exp(-20.4\text{kJ/mol}/RT)$ cm^3s^{-1}, and $k = 2.0\times10^{-10}exp(-49.1\text{kJ/mol}/RT)cm^3s^{-1}$, respectively. The rate constants for Ni were found to be pressure dependent at low temperatures suggesting a termolecular reaction.

ACKNOWLEDGMENTS

I would like to take this opportunity to recognize and thank the people whose assistance and guidance made this project possible.

First, I give heartfelt thanks to Associate Professor Mark Campbell, who suggested the project and has been very helpful in its completion. He spent numerous hours taking data with me in lab and was always willing to help solve problems and answer questions. I appreciate all the work he has done with me. In addition, I would like to recognize Midn. 1/C Kelli Hooper who has given much help and support to my research efforts.

I give my undying gratitude to Associate Professor Carl Wick who helped to restructure the computer program after the system crashed. Associate Professor Jeffrey Fitzgerald was very accommodating and helpful with the use of his glove box. Also, I'd like to thank Assistant Professor William Heuer for supplying $Cr(CO)_6$. I cannot forget the help of the machinists in the Rickover metal shop who were always willing to fix or make a piece of lab equipment.

Finally, I would like to thank the USNA administration for the providing the opportunity and facilities for such a project.

<u>Table of Contents</u>

INTRODUCTION

There are currently 109 known chemical elements which can be neatly arranged in the periodic table according to their electronic configurations. Each successive element has one more electron added to a subshell or shell of lowest energy. The transition elements consist of those elements in which electrons are added to the d subshell. Due to their lustre, malleability, conductivity and relatively low ionization energies, transition elements are all classified as metals.

In the on-going analysis of chemical kinetics, reactions of these transition metals have been of recent interest. With a broad range of properties, they play a key role in many chemical systems. Transition metals and their oxides are prevalent in meteors which break up in the Earth's atmosphere. Thus, when studying atmospheric chemistry their influence on atmospheric processes should be investigated.[1] In the age of computers, transition metals are also important. Their compounds are widely used as precursors in chemical vapor deposition, a process used in making computer chips.[2] Transition metals also play a key role in biochemistry. They can form complexes with organic molecules and are used in many biological functions. For example, iron (Fe) is present in hemoglobin, and vitamin B_{12} contains cobalt (Co).[3] Transition metals also play a central role in numerous catalytic processes.

Currently there is much interest in research involving transition metals due to the presence of many low-lying electronic states. The influence of high multiplicities and of ground and low-lying excited states on the gas-phase reactivity of these metals in oxidation reactions has received much attention. With the data reported so far, it

appears that the multitude of states in these atoms have a large effect on the dynamics of their reactions. Previous studies using reactions between the first row of transition metal cations and hydrogen have proven that electron configuration and spin multiplicity have a pronounced effect on the reactivity and selectivity of the metal cations.[4]

The mechanisms for the abstraction of transition metals with oxygen containing reactants are not yet well established. The resonance interaction model[5] and the electron transfer mechanism[6] have been used to model the depletion kinetics of transition metals in the presence of an oxidant. To calculate activation barriers, Fontijn and co-workers have developed an advanced resonance interaction model. This model uses correlations between the sum of ionization potential and s-p promotion energy (the energy needed to promote an s electron to the lowest p orbital which allows for partial sp hybridization) of various metals, the electron affinity of N_2O, the bond energy of the metal oxide bond and the rate constants of reactions of these metals with N_2O. The model has been tested for many main group metals; however, only a few experiments have been done with transition metals. For the main group metals, the model appears to adequately describe the reactions. Further studies are essential to determine the model's validity for transition metals.

In this study the primary goal was to perform a kinetic study of scandium (Sc), vanadium (V), chromium (Cr), cobalt (Co) and nickel (Ni) with nitrous oxide as a function of temperature and pressure:

$$TM + N_2O(X^1\Sigma^+) \rightarrow TMO + N_2.$$
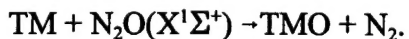
Results are reported in the following pages. The reactions of transition metals with nitrous oxide (N_2O) are all exothermic due to the formation of the stable nitrogen (N_2) and metal oxide molecules:[7]

	ΔH (kJ/mole)
$Sc + N_2O \rightarrow N_2 + ScO$	-505
$V + N_2O \rightarrow N_2 + VO$	-470
$Cr + N_2O \rightarrow N_2 + CrO$	-291
$Co + N_2O \rightarrow N_2 + CoO$	-201
$Ni + N_2O \rightarrow N_2 + NiO$	-206

Even though these reactions are all exothermic, and thus thermodynamically favorable as written, they are not expected to be very fast. Significant activation barriers have been found to exist in the reaction of N_2O with several metals.[8-14]

Temperature-dependent studies have previously been done for Ti[8], Cr[9] and Cu[10] with N_2O to determine their rate constants and thus the applicability of Fontijn's resonance model. Cr and Cu showed good correlation to the model's predicted activation energy (E_a), but the experimental value for Ti was over 50% greater that the experimental prediction. Recent experiments involving Mo[11], Fe[12] and Mn[13] with N_2O gave results inconsistent with Fontijn's calculated values. The reaction of W[14] with N_2O, however, is compatible with the resonance model. This research suggests that the resonance model is not consistently accurate for transition metal atoms most likely due to the fact that it does not account for the effects of outer shell d electrons.

In this paper, rate constants and Arrhenius parameters of reactions involving Sc, V, Cr, Co and Ni with N_2O as a function of temperature and pressure are reported (Table 1). Cr reactions have previously been observed and recorded and serve as a control for this study. These values for Sc, V, Co and Ni complete a study of the first row transition metals and their correlation to Fontijn's calculated values (Table 2, Figure 18). This report of rate constants and Arrhenius parameters adds to the database available to provide a better understanding of gas-phase kinetics of transition metal reactions.

EXPERIMENTAL

Reaction rates were determined as a function of temperature and pressure using a laser photolysis/ laser-induced fluorescence technique under pseudo first-order conditions ($[TM] << [N_2O]$). Sc, V, Cr, Co and Ni atoms were produced by photodissociation of transition metal precursors: $Sc(hfa)_3$, $Sc(TMHD)_3$, $V(CO)_6$, $V(CO)_4(C_5H_5)$, $V(C_5H_5)_2$, $Cr(CO)_6$, $Co(C_5H_5)(CO)_2$ and $Ni(C_5H_5)_2$ where hfa represents the hexafluoroacetylacetanato ion, and TMHD is the tris(2,2,6,6-tetramethyl-3,5-heptanedionato) ion. A diagram of the experimental arrangement is included as Figure 1. The photolysis laser is a Lambda Physik Lextra 200 with typical energy output of 100-300 mJ at 248 nm. The output of this excimer laser was used to photodissociate the precursor molecules in order to produce metal atoms in the reaction chamber. In some cases the laser output was focused in order to improve the signal. The reaction cell is a 5 cm i.d. stainless steel cross with attached sidearms and a sapphire window for optical viewing. This cell is contained in a commercial convection oven (Blue M, model 206F) which can attain temperatures up to 350 °C to allow for the measurement of the temperature dependence of the rate constants. The chamber temperature was measured using a thermocouple.

The precursor was entrained in a stream of N_2 buffer gas which flowed into the reaction chamber. Gas flows of the precursor, buffer gas and N_2O were regulated using mass flow controllers and flow meters. A slow flow of buffer gas was passed over the windows on each side arm in order to prevent a build-up of metal atoms and other photolysis products products on the surface of the window. The buffer gas was

used to regulate the total pressure in the chamber. Pressures were measured using MKS Baratron capacitance manomers. Partial pressures of the individual reactants were calculated using relative flows of the gas and the total pressure in the chamber.

Ground state and low-lying excited state atoms were detected via laser-induced fluorescence (LIF) using the output of an excimer pumped dye laser. The dye laser is a Lambda Physik Scanmate pumped by a Lextra 50. The Scanmate along with a Lambda Physik frequency doubling KDP crystal provided a 270 nm to 800 nm wavelength range for examination. Dye laser energies in the 100 - 1000 µJ range were obtained using this arrangement. The dye laser was used to excite the transition metal atom, and its fluorescence was then monitored by a Hamamatsu R375 photomultiplier tube placed perpendicular to the counterpropagated laser beams. The LIF decay consisted of 200 points in which each point was averaged over at least four laser pulses. The LIF signal was proportional to TM number densities. This LIF signal was subsequently sent to a gated boxcar sampler (Stanford Research Systems SR250), where the digitized output was analyzed and stored by a computer.

Atoms were observed via LIF using the eximer pumped dye laser. Ground state scandium was observed using the $y^2D_{3/2} - a^2D°_{5/2}$ transition at 402.042 nm.[15] Vanadium atoms were found using $a^4F_{3/2} - y^6F°_{1/2}$ transition at 403.284 nm to excite the electrons and using a 450 broadband filter to measure the fluorescence of the $y^6F°_{1/2} - a^6D_{3/2}$ transition.[15] Atomic chromium was observed using the transition $a^7S_3 - z^5P°_2$ at 373.080 nm while observing the fluorescence of the $z^5P°_2 - a^5S_2$ transition with a 520 narrowband filter.[15] Cobalt atoms were excited using the $a^4F_{9/2} - a^4G_{11/2}$ transition at

341.264 nm[15] and measuring the relaxation with a UG-1 filter. Ni atoms were also observed with a UG-1 filter. Ni (a^3D_3) was measured using a transition at 341.477 nm and Ni (a^3F_4) atoms was observed using a transition at 339.089 nm.[15] It is advantageous to choose transitions in which the exciting frequency of the atoms is different than the monitoring frequency of those atoms emitting. The benefit is that when the LIF is measured at a different wavelength than the laser uses, scattered background light is filtered out. If the scattered light signal was very strong, a neutral density filter was added to the eximer laser to reduce the amount of background interference in the signal.

The reaction time was determined as the time between the photolysis pulse and the dye-laser pulse. This delay was varied by a digital delay generator (Stanford Research Systems DG535). A delay of a few microseconds, usually 2-10 μs, was required to allow relaxation of highly excited atoms produced by the photolysis of the precursor molecules. After this delay, it was found that the small fraction of atoms still in the excited state did not affect the kinetic analysis for V or Sc. For Cr, Co and Ni a delay of one or two lifetimes was necessary to allow atoms to relax to the ground state. The trigger source was scattered pump laser light incident upon a fast photodiode. Data was taken over a time period of approximately three lifetimes for each reaction.

The following materials were used: N_2O (MG Industries, Electronic Grade, 99.999%), CH_4 (Linde Specialty Gas, 99.999%), N_2 (Potomac Airgas, Inc., 99.998%), SF_6 (Air Products, commercial grade). The precursors were Sc(hfa)$_3$ (Strem

Chemicals, 99.9%), Sc(TMHD)$_3$ (Strem Chemicals, 99%), V(CO)$_6$ (Strem Chemicals, 97%), V(CO)$_4$(C$_5$H$_5$) (Strem Chemicals, 97%), V(C$_5$H$_5$)$_2$ (Strem Chemicals, 95%), Cr(CO)$_6$ (Aldrich Chemical Co., 99%), Cr(CH$_3$COCHCOCH$_3$)$_3$ (Strem Chemicals, 97.5%), Cr(C$_6$H$_6$)$_2$ (Strem Chemical, 97%), CrO$_2$Cl$_2$ (Strem Chemicals, 99.%), Co(C$_5$H$_5$)(CO)$_2$ (Strem Chemicals, 98%) and Ni(C$_5$H$_5$)$_2$ (Strem Chemicals, 99%). The Cr(CO)$_6$ was obtained courtesy of Prof. Heuer.

state atoms. The non-exponential behavior is attributed to the relaxation of these higher excited states to the ground state. To determine $1/\tau$ for these plots, the exponential fit was done to data taken after one or two lifetimes. The length of the line in the logarithmic plot gives the range over which the data was analyzed.

The observed second order rate constant was calculated from a plot of $1/\tau$ versus N_2O pressure as shown in Figure 10 for $V + N_2O$, Figure 11 for $Sc + N_2O$, Figure 12 for $Cr + N_2O$, Figure 13 for $Co + N_2O$, and Figure 14 for $Ni + N_2O$. $Ni + N_2O$ was found to show pressure dependence; a graph of $1/\tau$ versus temperature is shown in Figure 15. In each of these plots, the solid line is a linear regression fit to the data in which the slope is equal to k_{2nd}. The intercept was found to be non-zero due to the sum of reactions with the precursor, other photolysis products and diffusion of TM atoms out of the detection zone. The bimolecular rate constants for each temperature are listed in Table 1. Absolute uncertainties are estimated at $\pm 30\%$ based on the sum of statistical scatter in the data, and uncertainty in the flowmeter readings (5%) and pressure readings (1%). For Sc, V, Cr and Co, the rate constants were found to be independent of pressure, thus indicating a bimolecular abstraction channel.

An Arrhenius plot was obtained using the following equation:

$$[\ln k_{2nd} = \ln A - (E_a/RT)]$$

Arrhenius plots for Sc, V, Cr and Co $+ N_2O$ are shown in figure 16. A plot demonstrating the non-Arrhenius behavior of $Ni + N_2O$ is shown in figure 17. The solid lines through the data are linear regression fits to the data. Measured rate constants andArrhenius parameters are given in Table 1.

Sc + N₂O

Two different precursors were employed in the study of Scandium with N_2O.

The first, Sc(hfa)₃ was only useful to a temperature of 473K. At higher temperatures

the signal became weak and an adequate signal could not be maintained to take

reliable data. The Sc(TMHD)₃ gave a strong signal at higher temperatures, but due to

a low vapor pressure, this compound had to be heated prior to entering the chamber.

Using a metal chamber, heating tape and heating mantle, the compound was raised to

a temperature of approximately 398K. This gave a sufficient vapor pressure to

introduce Sc precursor molecules into the chamber.

The photodissociation of the Sc(TMHD)₃ precursor occurred with very low

laser energy. The Sc(hfa)₃ compound took UV laser fluences of about 1 J/cm^2

whereas the Sc(TMHD)₃ compound could produce atoms with a considerably lower

laser fluence. Initially, the Sc(TMHD)₃ precursor was found to give different results

when compared to the rate constants given by the Sc(hfa)₃ compound at the same

temperature. The rate constants measured using Sc(TMHD)₃ were smaller with larger

time constants. This disparity is probably due to the production of excited state atoms

in the photodissociation of the Sc(TMHD)₃ compound. It was concluded that the

relaxation of the excited states occurred on the same time scale as the removal of the

ground state due to reaction with the N_2O and was thus interfering in the accurate

measurement of the rate constants of the ground state with N_2O. Therefore, rate

constants found by the Sc(TMHD)₃ were considered unreliable. Methane was added

to the chamber and was found to sufficiently quench the excited states on a short time scale without reacting with the ground state itself. Therefore, in the presence of methane, the excited states were quenched must faster than the decay of the ground state in the presence of N_2O. A partial pressure of methane of up to 12 Torr was used for experiments using this precursor. Even with methane as a quencher, however, the decay plots still showed growth in the beginning as shown in figure 6. A delay of about one lifetime was used before data was analyzed. The results subsequently obtained with the $Sc(TMHD)_3$ in the presence of methane were compatible with previous data taken using the $Sc(hfa)_3$ compound.

With these precursors, only rate constants in a temperature range of 298 - 523K were measured. At higher temperatures, the precursor was found to thermally decompose and an adequate signal could not be maintained. However, these measurements are sufficient to determine the activation energy for the reaction.

The activation energy for Sc was measured as 11.7kJ/mol. This is a 160% difference from the calculated value of 4.5kJ/mol using Fontijn's model.[5]

$V + N_2O$

Three precursors were employed for the analysis of V and N_2O. The $V(CO)_6$ was satisfactory; however, $V(CO)_4(C_5H_5)$ gave less scatter in the decay plots. Over the temperature range of 298 - 448K, a strong signal could be maintained with suitable time constants. At a temperature of 498K, however, the $V(CO)_4(C_5H_5)$ gave a weak signal. $V(C_5H_5)_2$ was used for the range of 498 - 523K. This precursor gave a

strong signal with slight heating to about 65°C. No other precursors were available to measure the rate at higher temperatures; however, the existing data is sufficient for determination of activation energy.

A value of 10.7kJ/mol was calculated for $V + N_2O$. This is 32% different than the calculated value of 8.1kJ/mol from the resonance interaction model.[5]

$Cr + N_2O$

Reactions of chromium with N_2O have already been studied.[9] The measurement of rate constants and activation energy done in this experiment was to serve as a control for the other elements studied here. Over a range of 298 - 523K, the results we were able to obtain agree with those previously measured. Thus, this method is within the experimental uncertainty of the other results.

$Cr(CO)_6$ was found to work well for a temperature range of 298-523K. However, at higher temperatures the signal was inadequate for data analysis. Several other compounds were employed with no success. Chromium (III) acetylacetonate, $Cr(CH_3COCHCOCH_3)_3$ gave a photolysis signal; however, no chromium atoms were produced to get an LIF signal. Even with heating, a signal could not be found. This may be attributed to the fact that the laser energy was not strong enough to break apart the precursor molecules. CrO_2Cl_2 also gave a signal; however, the liquid was very volatile and did not last long. Also, with this precursor, very short lifetimes were obtained prior to introduction of N_2O, $\tau=6.2$ μs at 548K. A plot using this data would be unreliable due to such short time constants. $Cr(C_6H_6)_2$, was also tried with no

success. Again a photolysis signal was obtained, but no LIF signal could be found. The oven temperature was then lowered to below 500K and $Cr(CO)_6$ was introduced into the system. With these conditions, a signal could be found with the $Cr(CO)_6$. This suggests that the other precursors were unsuccessful and that the experimental set up was still reliable.

The value of activation energy calculated for $Cr + N_2O$ was 20.4 kJ/mol. This agrees with the calculated value of 20.8 kJ/mol predicted by Fontijn's model.[5]

The main focus of this study was on the ground (a^7S_3) state; however, other excited (a^5D_J and a^5S_J) states were also studied to determine their effect on the decay profiles of the ground state. This was done by exciting the atoms at a wavelength of 520.474 nm for the Cr (a^5S_2) state, and wavelengths of 461.343 nm, 462.624 nm, 461.619 nm, 465.215 nm and 464.615 nm for the Cr (a^5D_0, a^5D_1, a^5D_2, a^5D_3, a^5D_4) states, respectively.[15]

The removal rate constants for the spin-orbit excited states were measured at 298K. All of the rate constants were found to be of the same order as the gas kinetic collision rate (1.4×10^{-10} cm^{3}s^{-1}), which is at least 3 orders of magnitude faster than the ground state reacts. These results are tabulated in Table 3. Thus, the spin-orbit excited states of chromium do not affect the measurement of ground state reactions. These states were difficult to measure, with a large amount of scatter in the data. Data were taken at a total pressure of 4 and 10 Torr, with partial pressures of N_2O over a range of 0.0 - 0.02 Torr.

Co + N₂O

Initially, the cobalt transition $z^6G_{11/2}$ - $a^4F_{9/2}$ was detected and excited using a wavelength of 391.1 nm. By measuring the LIF at this wavelength, a large signal of scattered light was obtained, and a only a small signal/noise ratio could be measured for the cobalt. Under these conditions, suitable data could not be accurately measured. At room temperature, $Co(C_5H_5)_2$ did not produce atoms in the reaction chamber. $Co(CO)_3NO$ had a high vapor pressure and was very volatile at room temperature. A strong signal was produced, but there was no reaction at 298K or 423 with N_2O. Before the temperature was raised, the signal began to fluctuate and the precursor was found to have evaporated. $Co(C_5H_5)_2$ gave a good signal; however, the lifetime was very short even without any N_2O. Short lifetimes cannot give a very accurate rate constant, therefore this precursor could not be used.

Using $Co(C_5H_5)(CO)_2$ gave good plots. This precursor had a high vapor pressure at room temperature and could be used at room temperature to produce atoms in the gas phase. A strong signal could be maintained using a wavelength of 341.264 nm; however, no reaction could be measured with $Co + N_2O$ at temperatures below 448K. Above 448K, the decay profiles exhibited growth at the beginning (Figure 8). Thus, determination of $1/\tau$ was done by an exponential fit to the decay profile after a delay of at least one lifetime. Data were taken over the range of 448K - 573K. Attempts were made to obtain rate constants at lower temperatures, but the rate constant was smaller than the lower limit of the apparatus under these conditions.

Even at higher temperatures, however, the rate constants were of a very small magnitude. To obtain observable decays of the ground state, a large partial pressure of N_2O was required. Thus, relatively high total pressures were necessary to allow for a large partial pressure of N_2O.

The activation energy was measured as 49.1 kJ/mol which is a difference of 55.9% from the value of 31.5kJ/mol calculated using the resonance interaction theory.[5]

Ni + N₂O

The Ni LIF transitions observed were the same transitions at which the atoms were excited. The decay rates of the a^3D_3, a^3F_4 states were studied as a function of temperature and pressure. Ni reactions were found to be pressure dependent at low temperatures, indicating a termolecular process. In a termolecular process, the rate constant is dependent on a third factor. In this reaction, the number density of the buffer gas, $[N_2]$, affects the rate of the reaction.

$$Ni + N_2O \xrightarrow{[N_2]} NiON_2$$
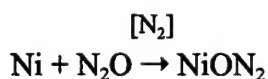
When the molecules collide with the N_2, they transfer energy, thus affecting the rate.

At higher temperatures, however, the abstraction channel becomes more important. Rate constants were measured in a pressure range of 2.5 - 200 Torr over a temperature range of 298 - 623K. More research is necessary to determine the Arrhenius parameters and the mechanism for the reaction of $Ni + N_2O$.

The majority of the decay profiles for Ni + N_2O showed growth at the beginning. This is attributed to the relaxation of higher states and data was analyzed after approximately one lifetime. SF_6 was determined to be unreactive to the ground state and did marginally quench initial growth. Even with SF_6, however, some growth was still present. Data were analyzed after a delay of approximately one lifetime.

Two states of Ni were observed, the a^3D_3 and the a^3F_4 state. Rate constants are listed in Table 3 for each temperature and pressure. A plot of $1/\tau$ vs $[N_2O]$ gives a line in which the slope is the second order rate constant, k_{2nd}. For Ni, the plots show both a temperature dependence (Figure 14) and a pressure dependence (Figure 15).

Arrhenius plots are given in Figure 17. No curve could be drawn to adequately describe the behavior. Thus, no parameters were obtained.

DISCUSSION

Results show bimolecular abstraction channels for ground state Sc, V, Cr and Co. Ni was found to have a pressure dependence and more experiments are required in order to adequately describe the reaction.

All of the reactions of the transition metals with N_2O have negative enthalpies of reaction due to the formation of the stable N_2 molecule; thus, there are no thermodynamic barriers to the reaction. All reactions studied here, however, show reaction barriers, E_a. Unfortunately, there are no calculations available to describe the potential energy surfaces involving a transition metal and N_2O. Several theories have been promulgated, but more work with theoretical calculations needs to be done to explain this phenomenon.

The presence of this activation barrier has been attributed to the electron affinity of N_2O. There is an energy barrier between the excited and ground state which represents the energy necessary to bend the N_2O molecule.[16] Also the ground state of N_2O $(X^1\Sigma^+)$ correlates to excited $O(^1D_2) + N_2(^1\Sigma^+)$ which is 15,868cm^{-1} above $O(^3P_2)$.[17] To obtain low-energy product states, the surface must change from $O(^1D_2)$ to $O(^3P_2)$ character.[6] These surfaces are important for transition metals reactions because these elements have numerous low lying states corresponding to many accessible potential energy surfaces. The activation energy is based on the changing of surfaces to obtain accessible reaction channels.

Resonance theory was used by Futerko and Fontijn to explain the activation barriers to the TM + N_2O reaction. The activated complex $(N_2OTM)^{\ddagger}$ can be

described with three resonating structures. The first structure is a covalent bond between O and TM in which the TM uses the s orbital for bonding. The second structure is also a covalent bond, except the TM bond has p character. The last structure results from the interaction of N_2O^- and TM^+. The activation energy can then be calculated based on the wavefunctions of these structures and their contribution to the electronic structure. The resonance can be described as the superposition of the distinct wavefuctions of each resonance structure.[5] It is important to point out here that the calculations are based on the premise that the metal - oxygen bond is only of s and p character. The model does not account for the presence of d electrons of the transition metals or the electronic structure of the TM - O bond.

According to the resonance interaction theory, as the ionization potential and s-p promotion energy of the TM increase, the energy differences between the resonating structures should also increase. This causes the resonance energy to decrease and the activation energy to increase. The sum of ionization potential and s-p promotion energy follows a trend as follows: Co(1041kJ/mol) > Cr(932kJ/mol) > V(847kJ/mol) > Sc(818kJ/mol). The model predicts that the activation energies will follow the same trend. The activation energies found experimentally do not agree with this prediction. Co(49.1kJ/mol) > Cr(20.4kJ/mol) > Sc (11.7kJ/mol) > V (10.7kJ/mol). Therefore, the results of this experiment do not agree with Futerko and Fontijn's theory.

Table 2 presents a list of several transition metals with their experimental and calculated activation energies from the resonance interaction model. They are listed

in order of correlation to the resonance interaction model. As shown, this model does not consistently predict the activation energy for the transition metals. There does not seem to be a direct correlation between the E_a, the sum of the ioniztion potential and s-p promotion energy, the s-d promotion or the enthalpy of reaction. Those transition metals that showed the best correlation (< 10%) to the model's calculated values had relatively low s-d promotion energies. Those that varied the most from the calculated E_a (>100%) had relatively high energies for s-d promotions. These correlations, however, do not follow a consistent trend. More consideration is necessary to determine if a good model is possible for these reactions. Also, more theoretical calculations need to be explored to explain the interaction of the potential energy surfaces. A good model would be usedful to see if a correlation exists in order to calculate the activation energy for these reactions.

Reactions involving $Cr + N_2O$ were to serve as a control for the results. Rate constants and Arrhenius parameters have been previously measured for this reaction.[8] Recently, Fontijn, et al. reported an equation of $k(278 - 1150K) = 2.2 \times 10^{-12}$ $(T/K)^{0.55} \exp(-2851K/T)$ $cm^3 s^{-1} molecule^{-1}$; however, this equation is not consistent with the data they report. A better fit to the regression line is described by 2.23×10^{-12} $(T/K)^{0.53} \exp(-20.4kJ/mol/RT)$, which corresponds to results reported here.

SUMMARY

The bimolecular rate constants and Arrhenius parameters were measured for the ground states of Sc, V, Cr and Co with N_2O over a temperature range of 298K - 623K. Ni was determined to be pressure dependent at low temperatures. More research is required in order to accurately describe the reaction channel for the reaction of Ni + N_2O. The activation energies for these metals did not follow an increasing trend correlating to the sum of ionization potential and s-p promotion energy. This strengthens the argument that the resonance interaction model is not consistent for transition metals due to the presence of outer shell d electrons. Further parameters must be added to the equation in order to account for the effects of d electrons in the outer shell of the atom.
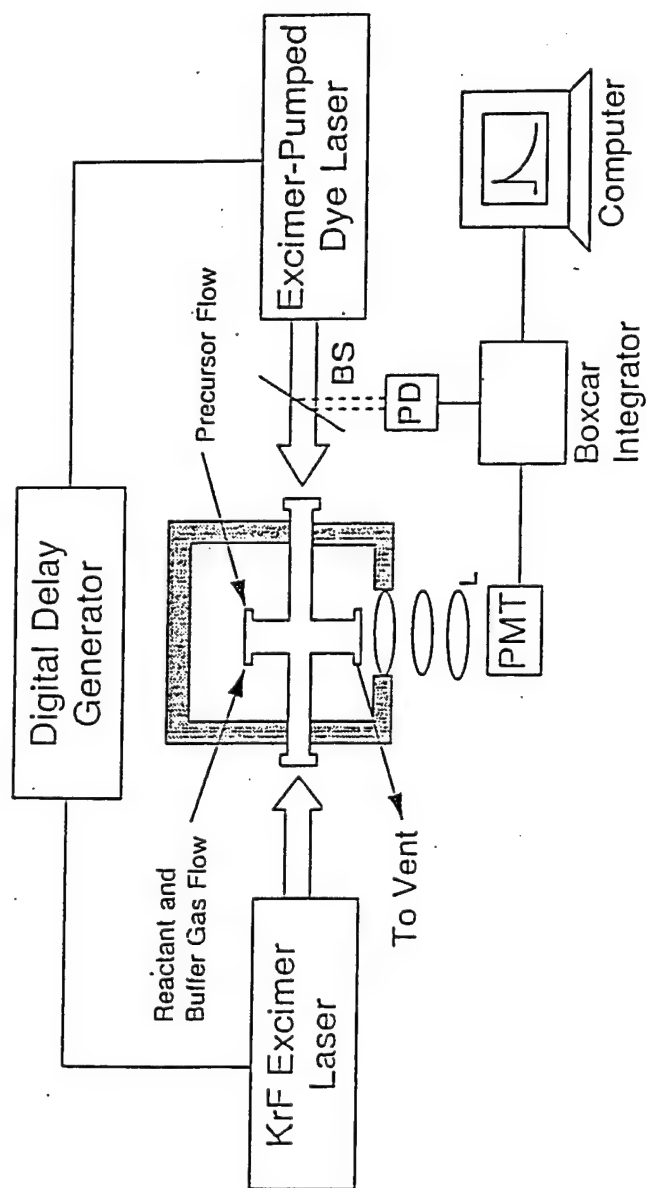
Figure 1. Illustration of the experimental setup used for reported studies. L is the lens, PMT is the photomultiplier tube, PD is the photodiode and BS represents the beam splitter.
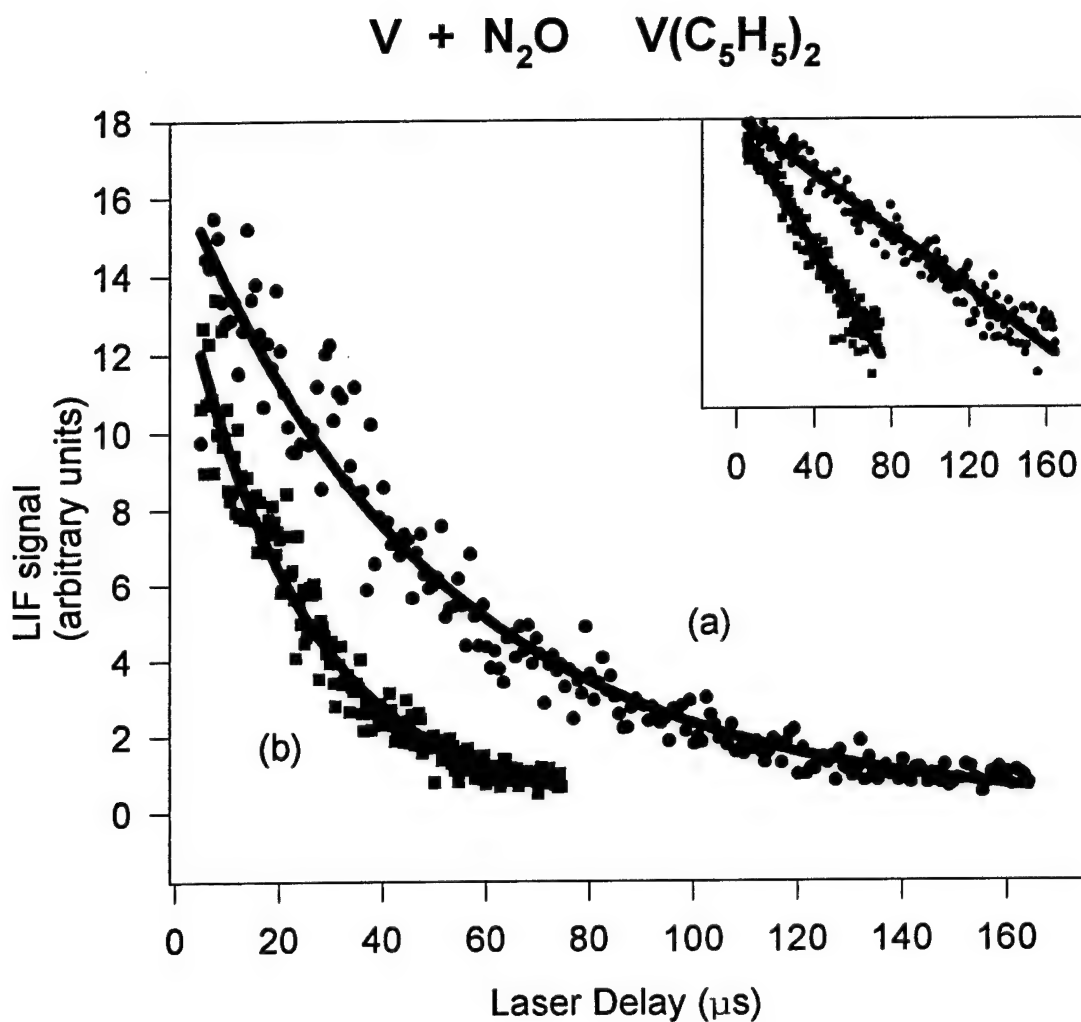
Figure 2. Typical decay profile for TM + N_2O. Data shown is for $V(C_5H_5)_2$, T = 498K, P_{total} = 20 Torr. Solid lines are exponential fits to the data with (a) $P(N_2O)$ = 0.0226 Torr, τ = 51.0 μs and (b) $P(N_2O)$ = 0.632 Torr, τ = 24.1 μs. The inset plot is a log fit to the data.
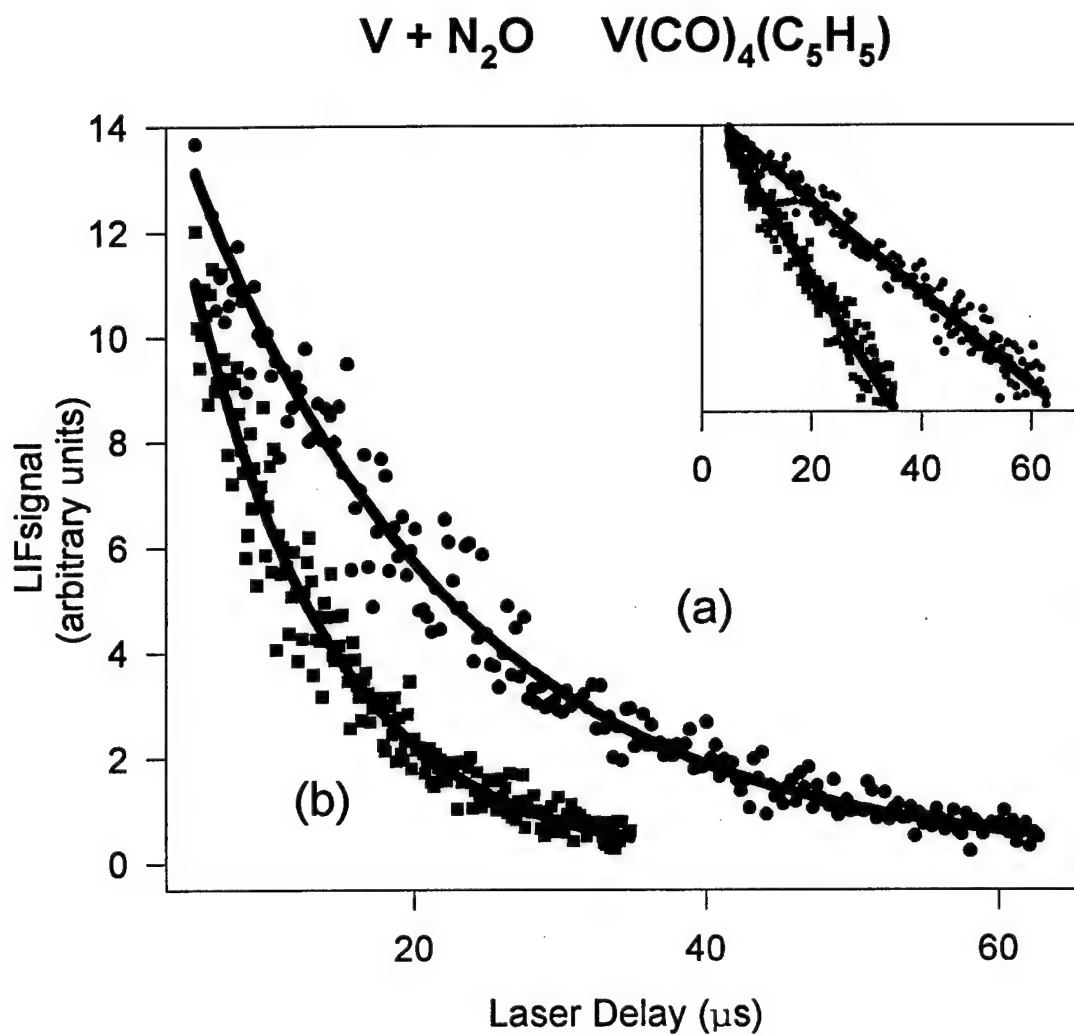
$$V + N_2O \quad V(CO)_4(C_5H_5)$$

Figure 3. Decay profile for $V(CO)_4(C_5H_5)$, T = 373K, P_{total} = 20 Torr. Solid lines are exponential fits to the data. (a) $P(N_2O)$ = 1.38 Torr, τ = 18.2 μs and (b) $P(N_2O)$ = 2.76 Torr, τ = 9.6 μs. The inset plot is a log fit to the data.
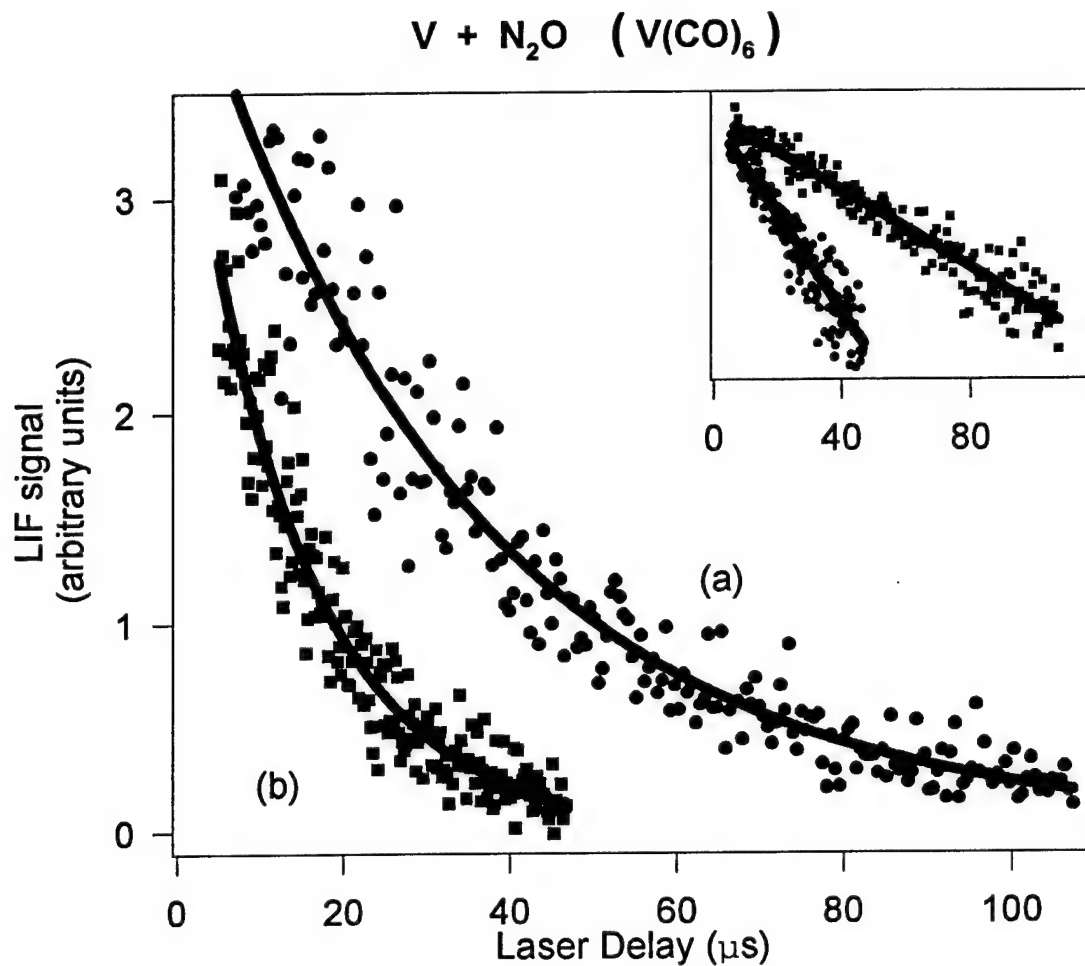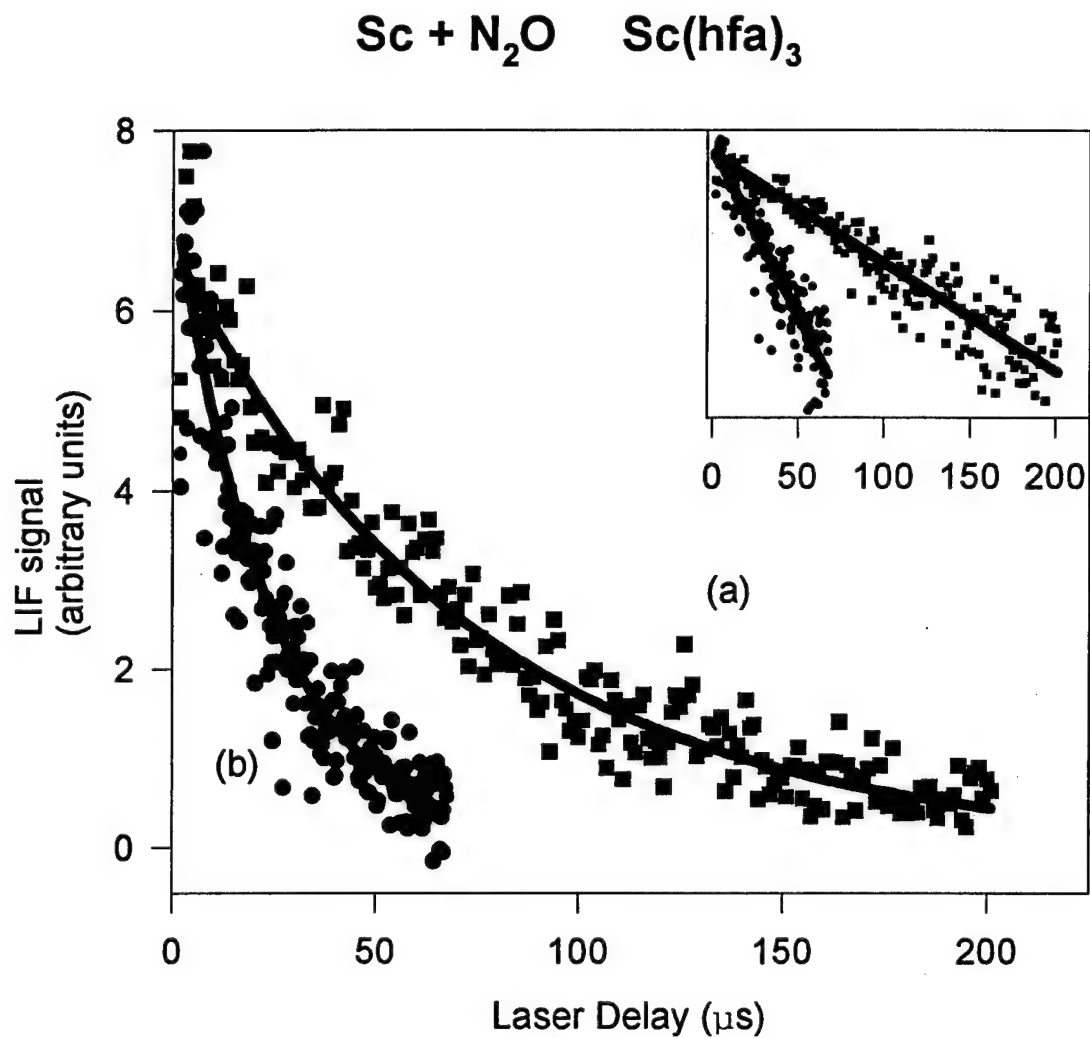
Figure 4. Decay profile for $V(CO)_6$, T = 295K, P_{total} = 20 Torr. Solid lines are exponential fits to the data. (a) $P(N_2O)$ = 1.91 Torr, τ = 26.57 μs and (b) $P(N_2O)$ = 3.81 Torr, τ = 13.2 μs. The inset plot is a log fit to the data.

Figure 5. Decay profile for Sc(hfa)$_3$, T = 299K, P$_{total}$ = 20 Torr. Solid lines are exponential fits to the data. (a) P(N$_2$O) = 0.0516 Torr, τ = 72.1 μs and (b) P(N$_2$O) = 0.723 Torr, τ = 23.1 μs. The inset plot is a log fit to the data.
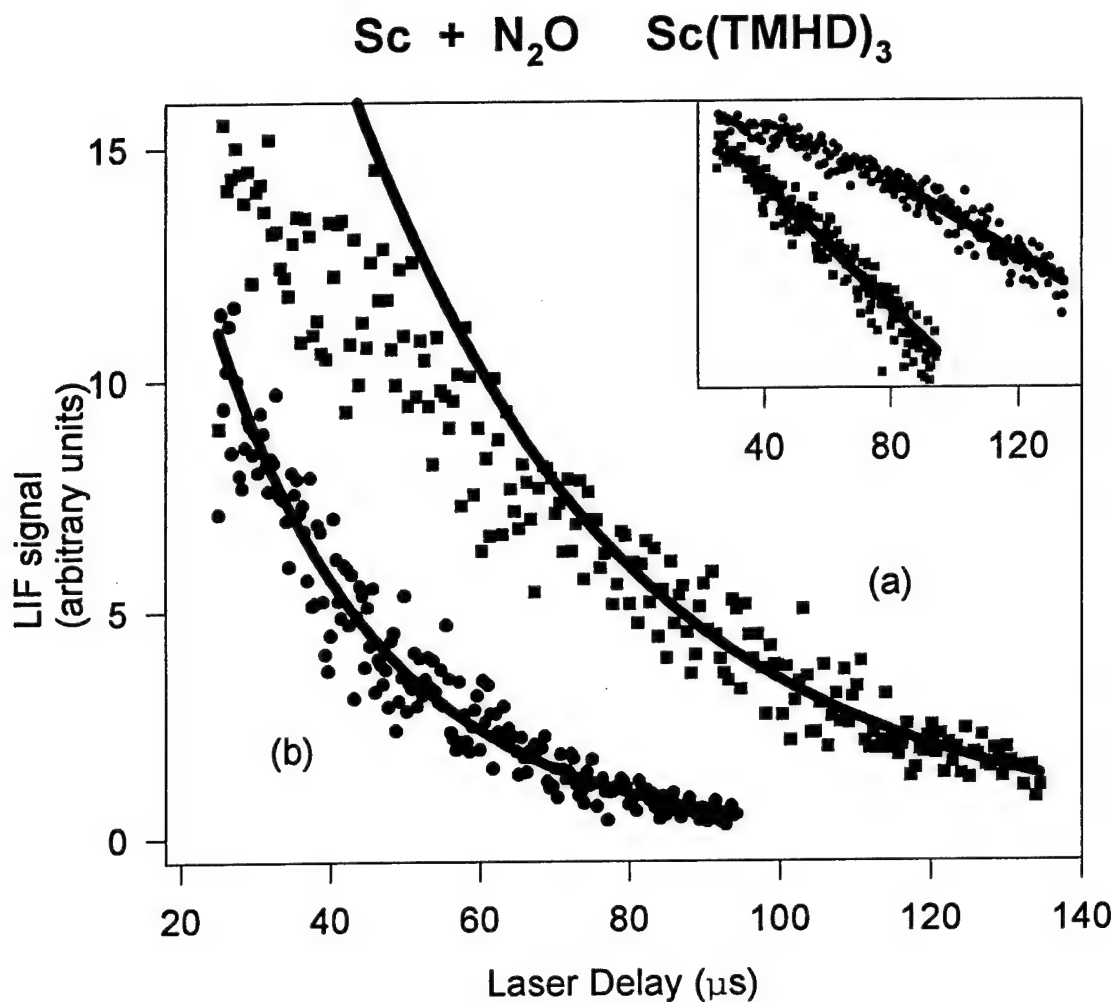
Figure 6. Typical decay profile for Sc(TMHD)$_3$, T = 523K, P$_{total}$ = 20 Torr.
Solid lines are exponential fits to the data after at least one lifetime.
CH$_4$ was used as a quencher, but growth is still present at the
beginning. (a) P(N$_2$O) = 0.013 Torr, τ = 43.1 μs and (b) P(N$_2$O) =
0.103 Torr, t = 21.3 μs. The inset plot is a log fit to the data. The
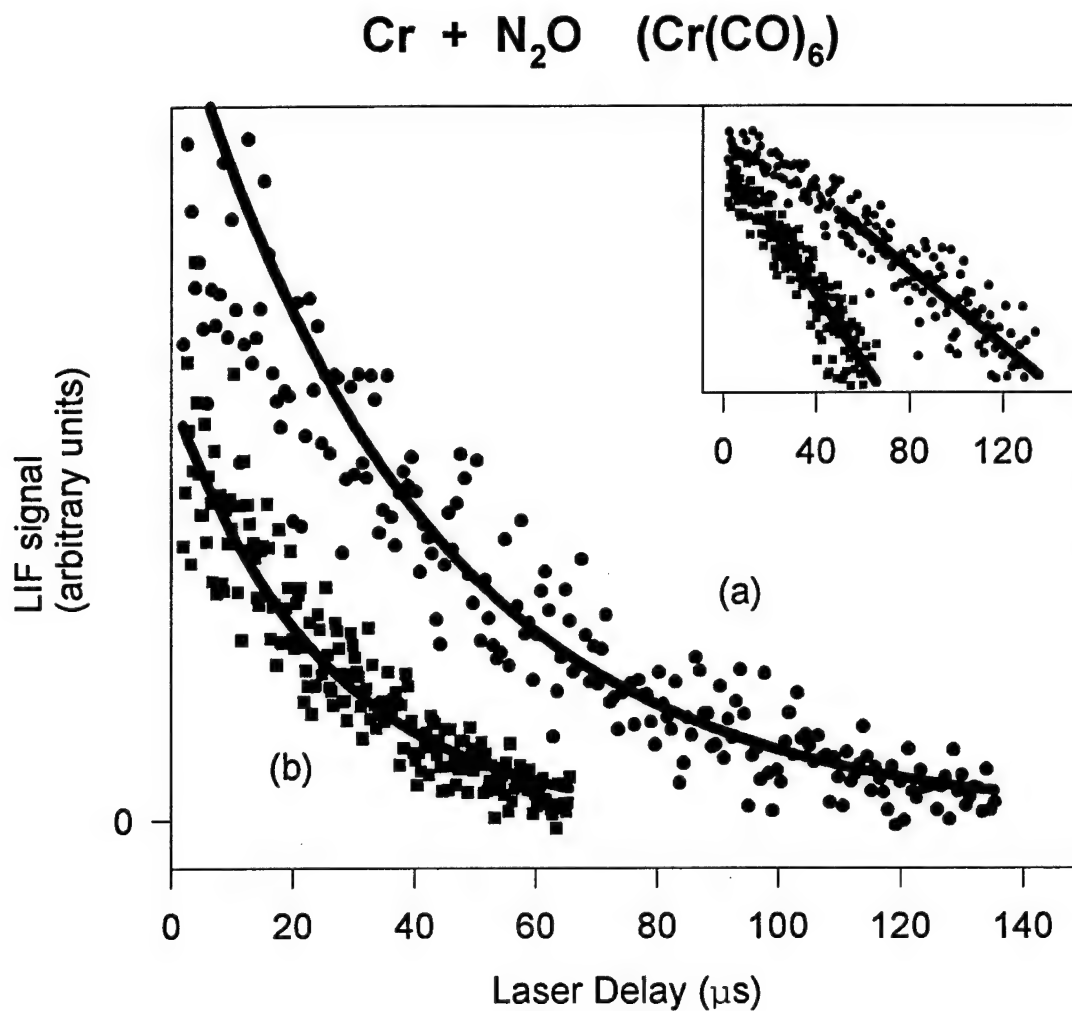solid line shows the range over which the data was analyzed.

Figure 7. Decay profile for $Cr(CO)_6$. T= 473K, P_{total} = 20 Torr. Solid lines
are exponential fits to the data. (a) $P(N_2O)$ = 2.44 Torr, τ = 61 μs
and (b) $P(N_2O)$ = 8.63 Torr, τ = 22.9 μs.
The inset plot is a log fit to the data.
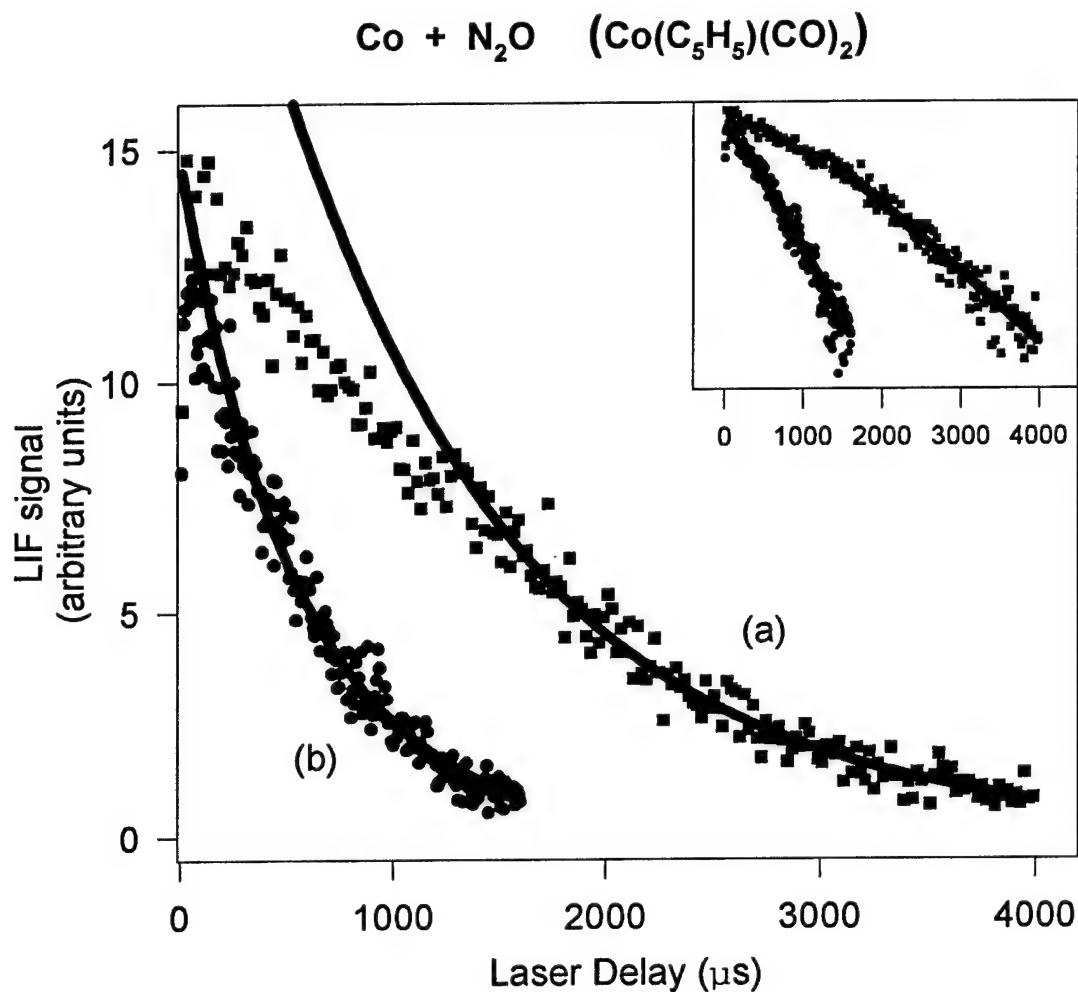
Figure 8. Typical decay plot for $Co(C_5H_5)(CO)_2$. T= 498K, P_{total} = 100 Torr. Solid lines are exponential fits to the data. (a) $P(N_2O)$ = 17.987 Torr, τ = 1133 μs and (b) $P(N_2O)$ = 61.8 Torr, τ = 512 μs. The inset plot is a log fit to the data in which the solid line is the range over which the data was analyzed.
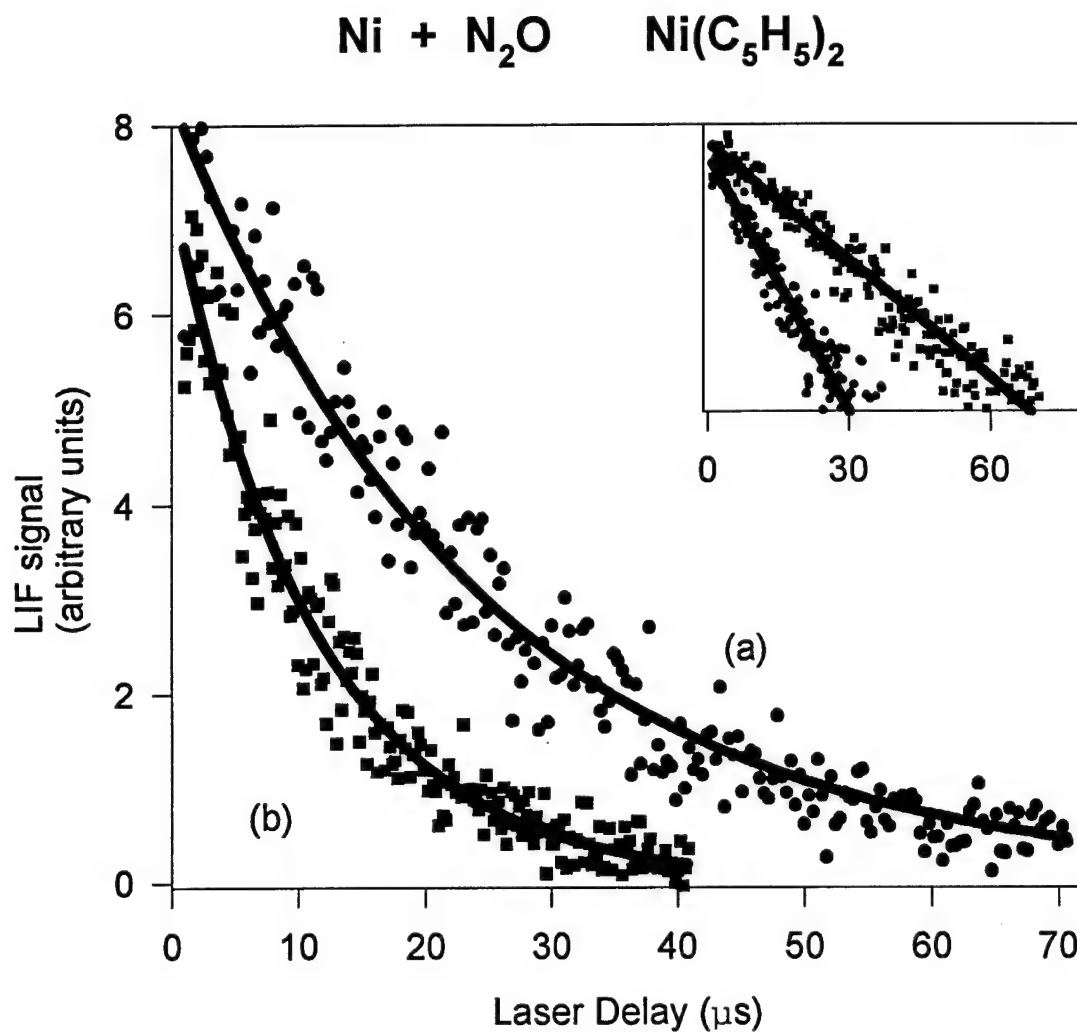
$$Ni \ + \ N_2O \quad Ni(C_5H_5)_2$$

Figure 9. Decay plot for $Ni(C_5H_5)_2$, SF_6 was used as a quencher. $T = 523K$, $P_{total} = 20$ Torr. Solid lines are exponential fits to the data. (a) $P(N_2O) = 12.7$ Torr, $\tau = 10.3$ μs and (b) $P(N_2O) = 6.31$ Torr, $\tau = 22.5$ μs. The inset plot is a log fit to the data.
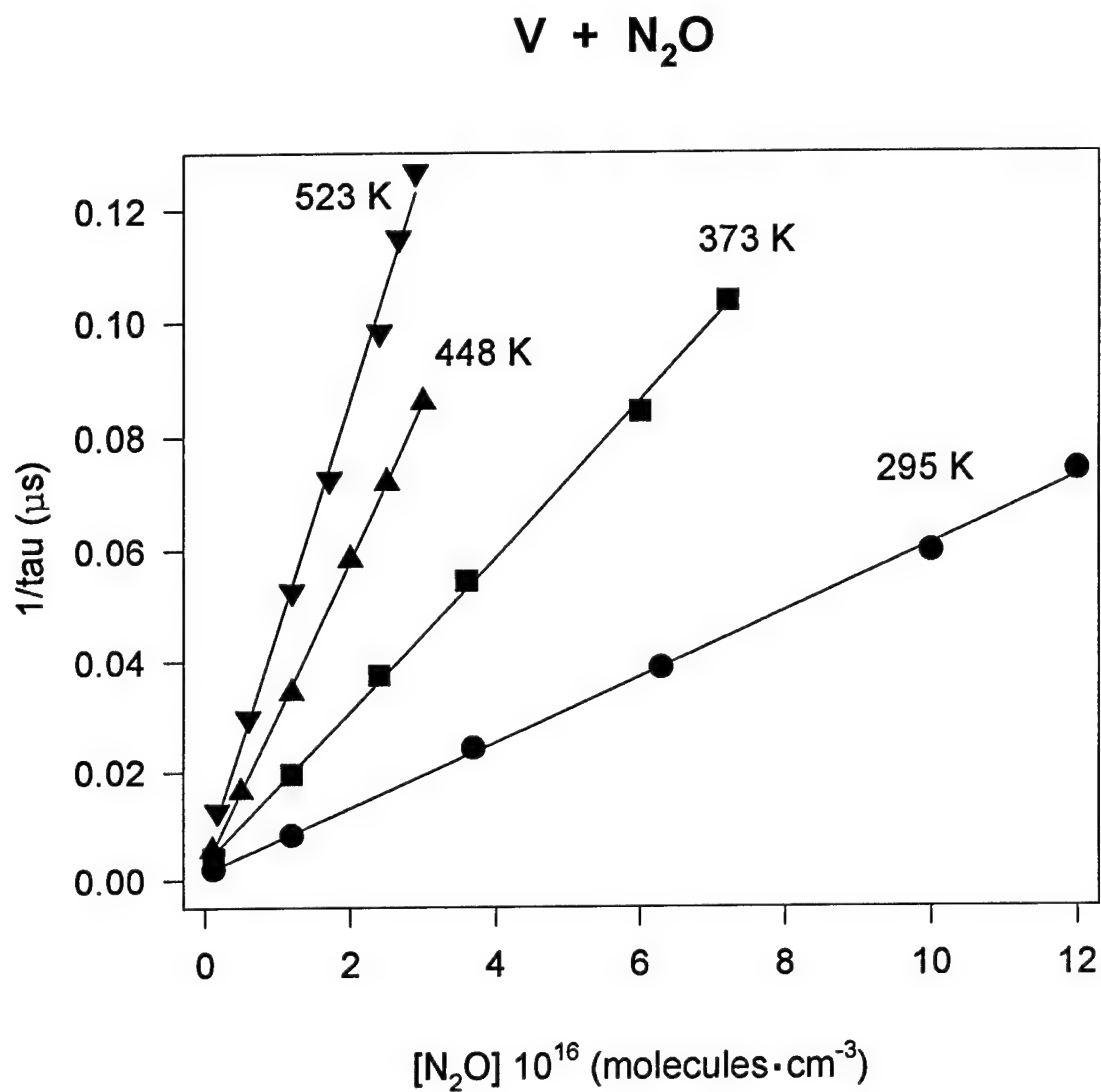
V + N$_2$O

Figure 10. Plot for determining the second-order rate constant, k$_{2nd}$, for V + N$_2$O. The slope of the regression line yields k$_{2nd}$ in cm^{3}s^{-1}.

Figure 11. Plot for determining the second-order rate constant, k_{2nd}, for Sc + N_2O. The slope of the regression line yields k_{2nd} in cm^3s^{-1}.

Cr + N₂O

Figure 12. Plot for determining the second-order rate constant, k_{2nd}, for Cr + N_2O. The slope of the regression line yields k_{2nd} in cm^3s^{-1}.

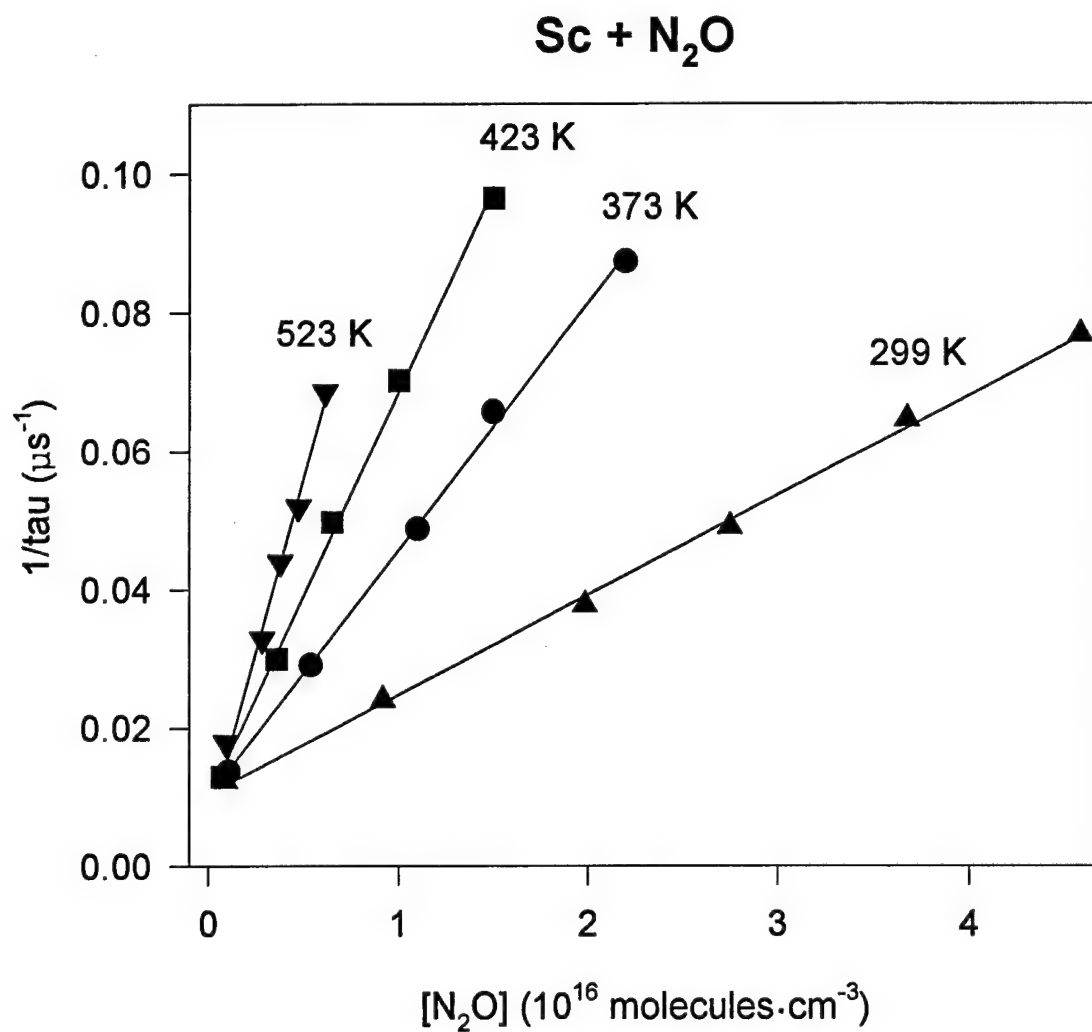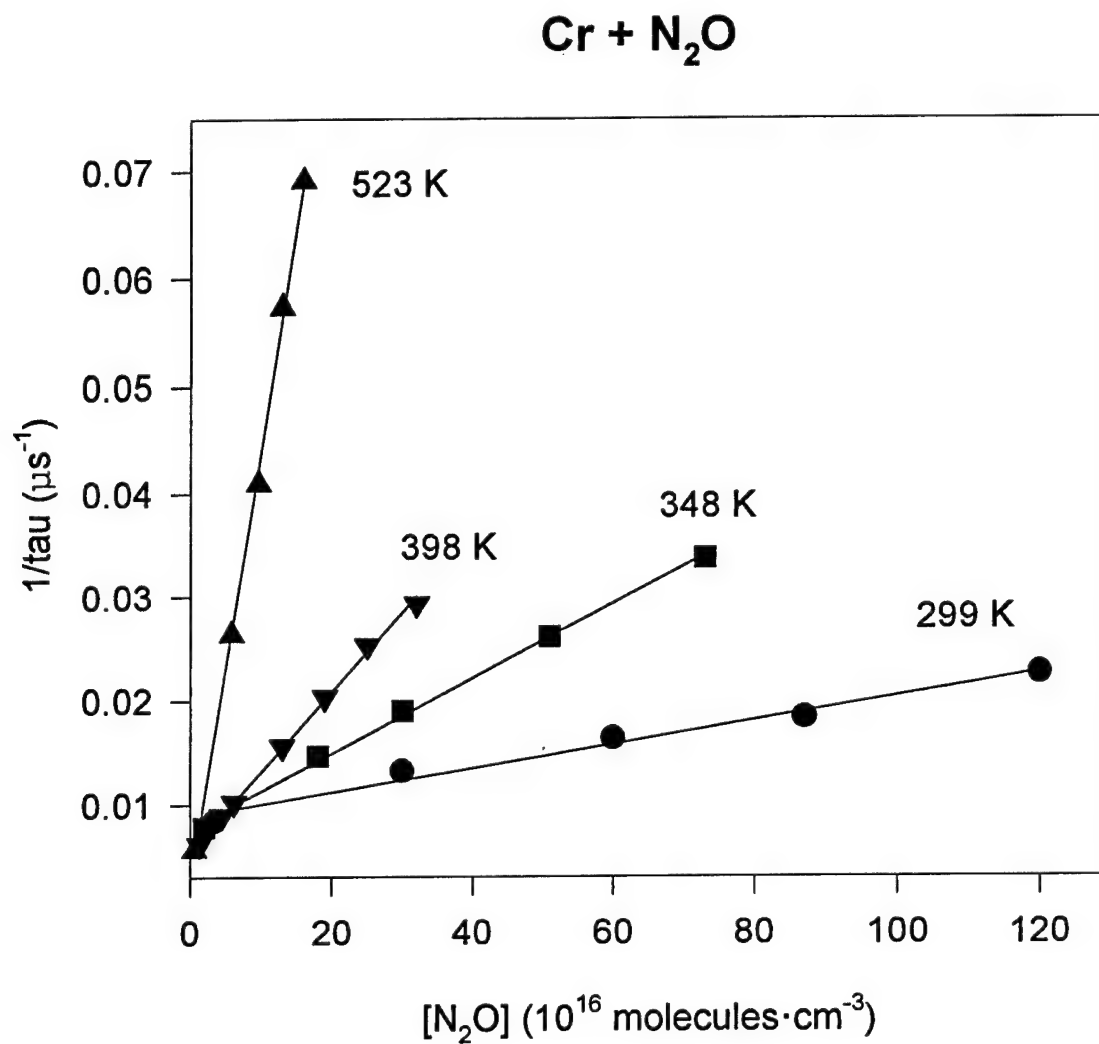**Figure 13.** Plot for determining the second-order rate constant, k_{2nd}, for Co + N_2O. The slope of the regression line yields k_{2nd} in cm^3s^{-1}.

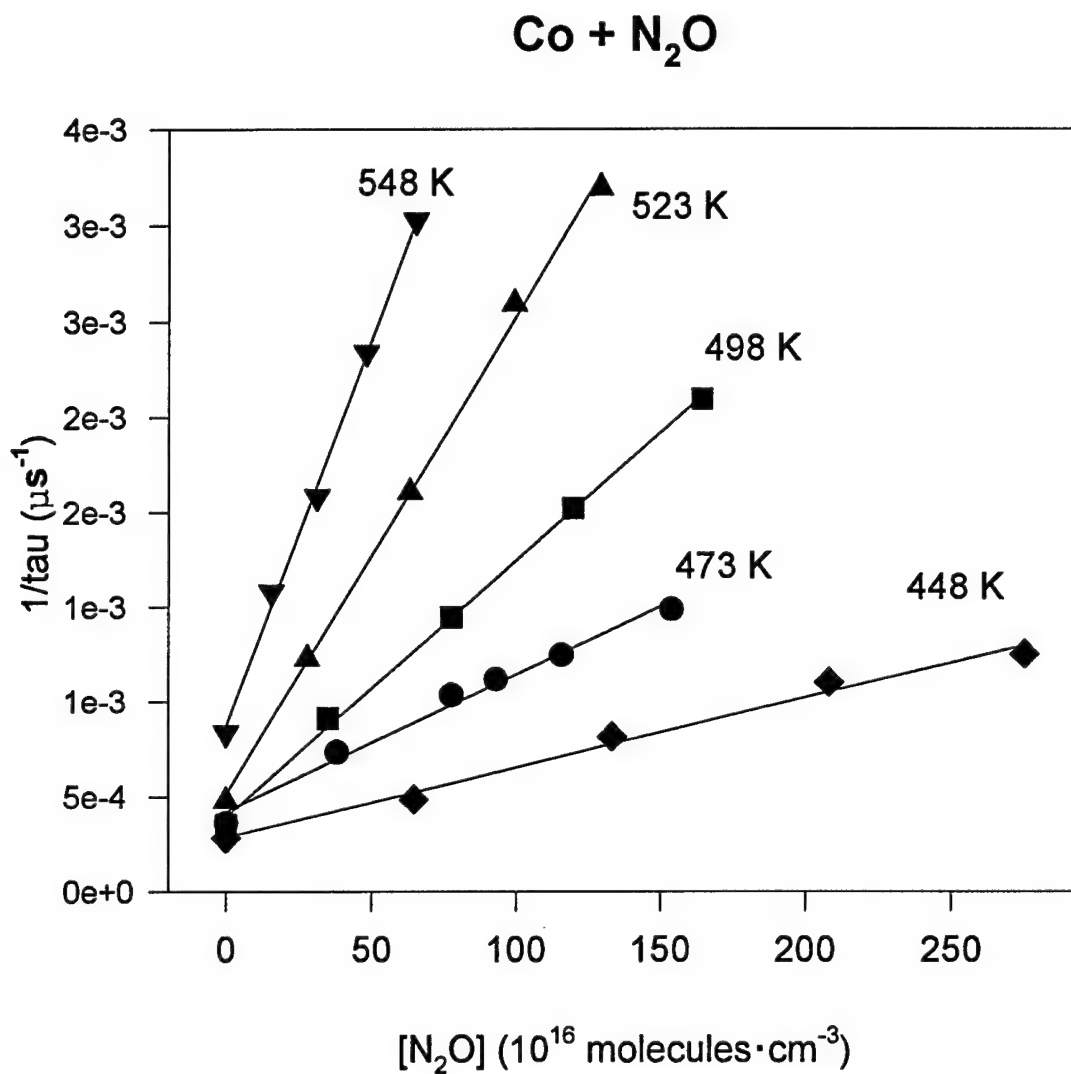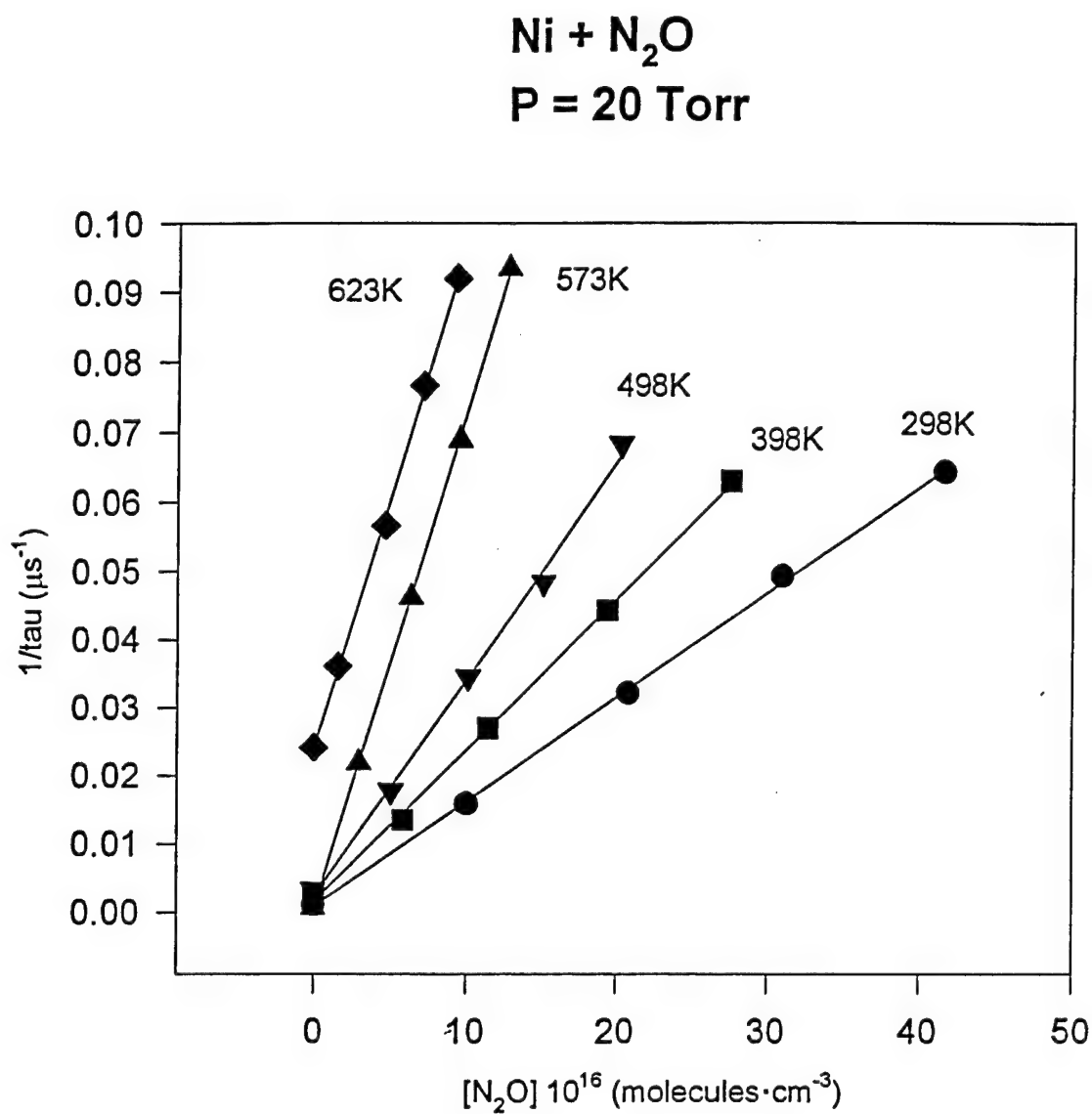**Figure 14.** Plot for determining the second-order rate constant, k_{2nd}, for Ni + N_2O as a function of temperature. The slope of the regression line yields k_{2nd} in cm^3s^{-1}.
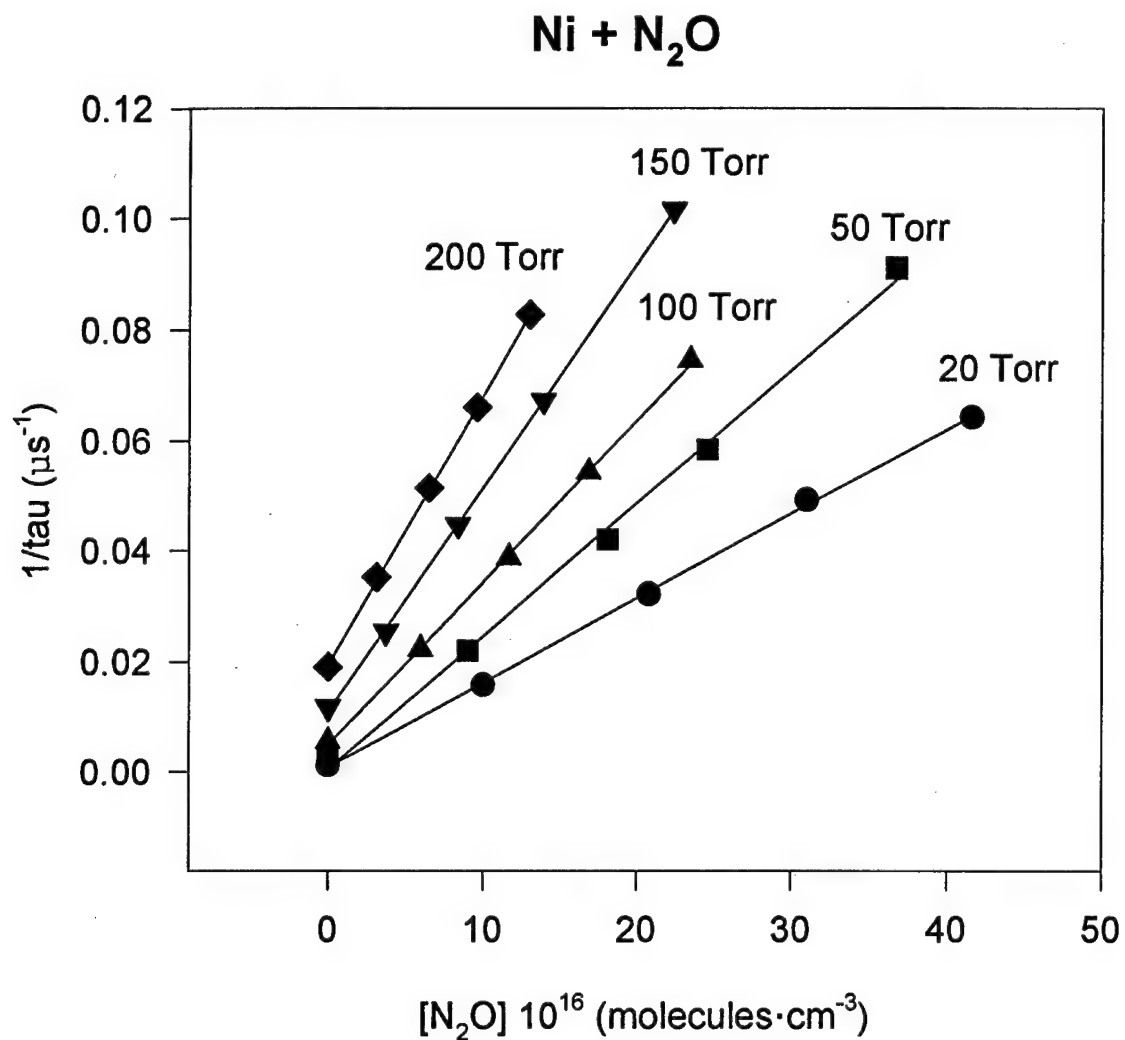
Figure 15. Plot for determining k_{2nd} as a function of pressure. As shown in the graph, Ni + N_2O was found to be pressure dependent. Data shown is for T = 298K. The slope of the regression line yields the second-order rate constant for each pressure.
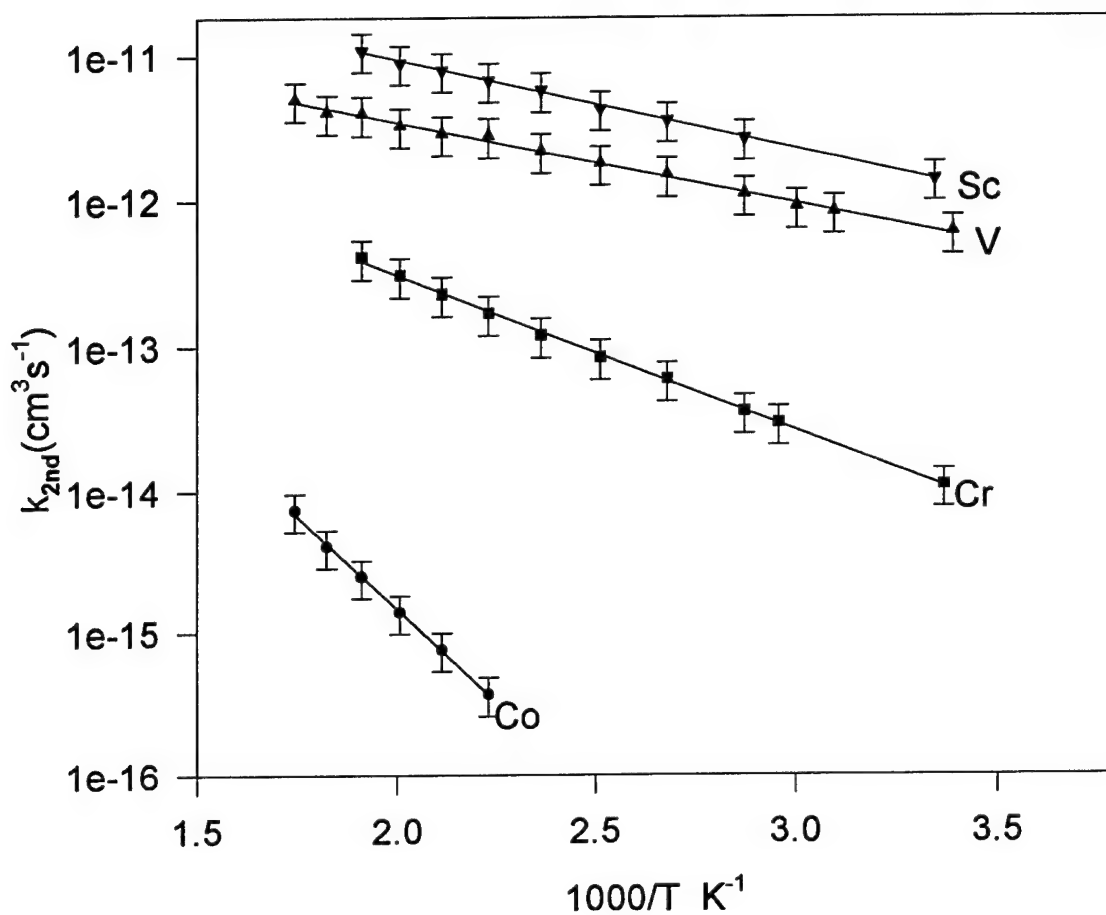
Figure 16. Arrhenius plots for Sc, V, Cr and Co + N_2O. The solid fit line through the data points is a regression line fit to the equation $k(T) = \exp(-E_a/RT)$. Error bars represent +/- 30% uncertainty.

Arrhenius Plot
Ni (a^3D_3) + N_2O
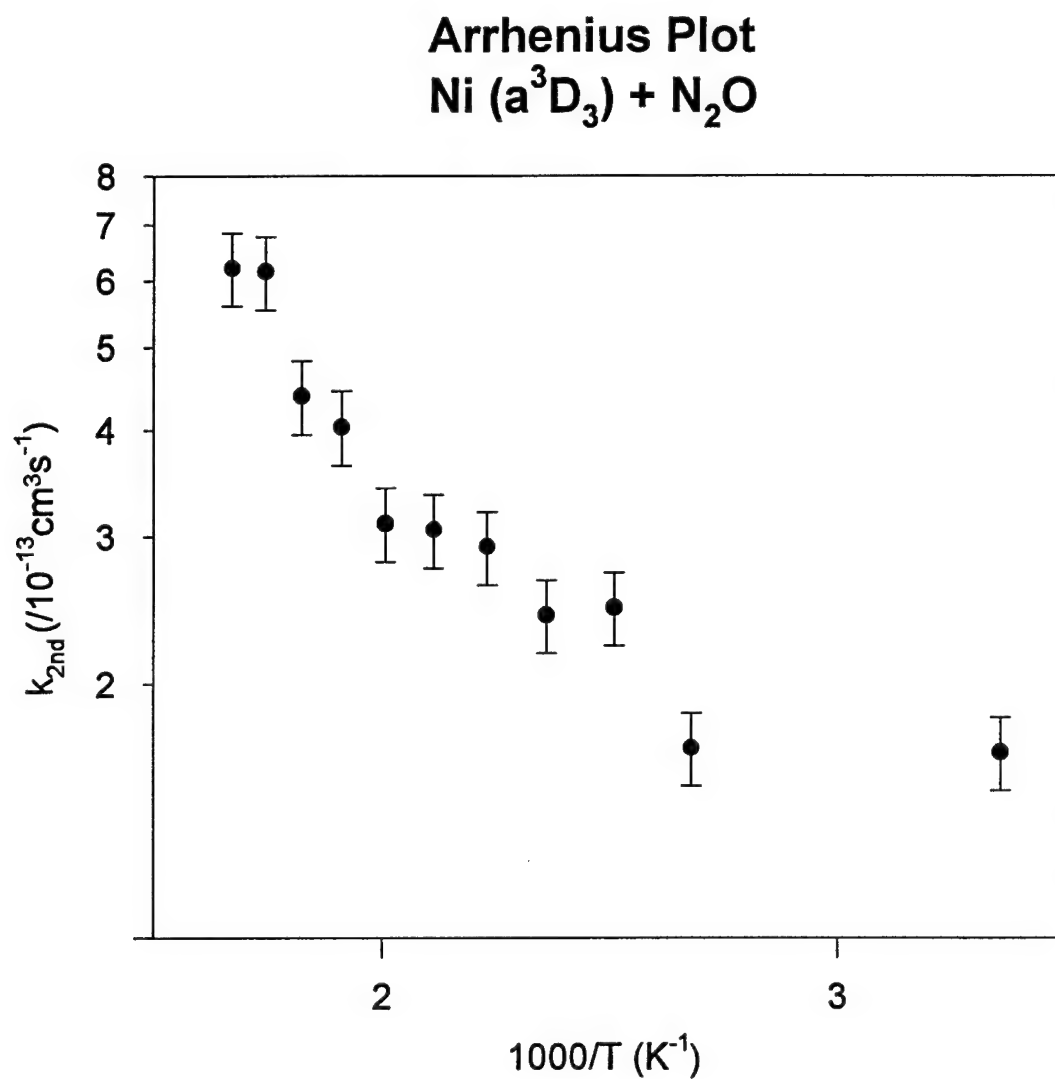
Figure 17. Arrhenius plot for Ni + N_2O showing pressure dependence at low temperatures. Error bars represent +/- 10% uncertainty.

Figure 18. Comparison of experimental and resonance interaction models's calculated Ea's versus the sum of s-p promotion energy and ionization potential. The solid squares are calculated values, while the double triangles represent experimental values. The solid line is a regression fit to the calculated data.

Table 1. Rate Constants and Arrhenius parameters.
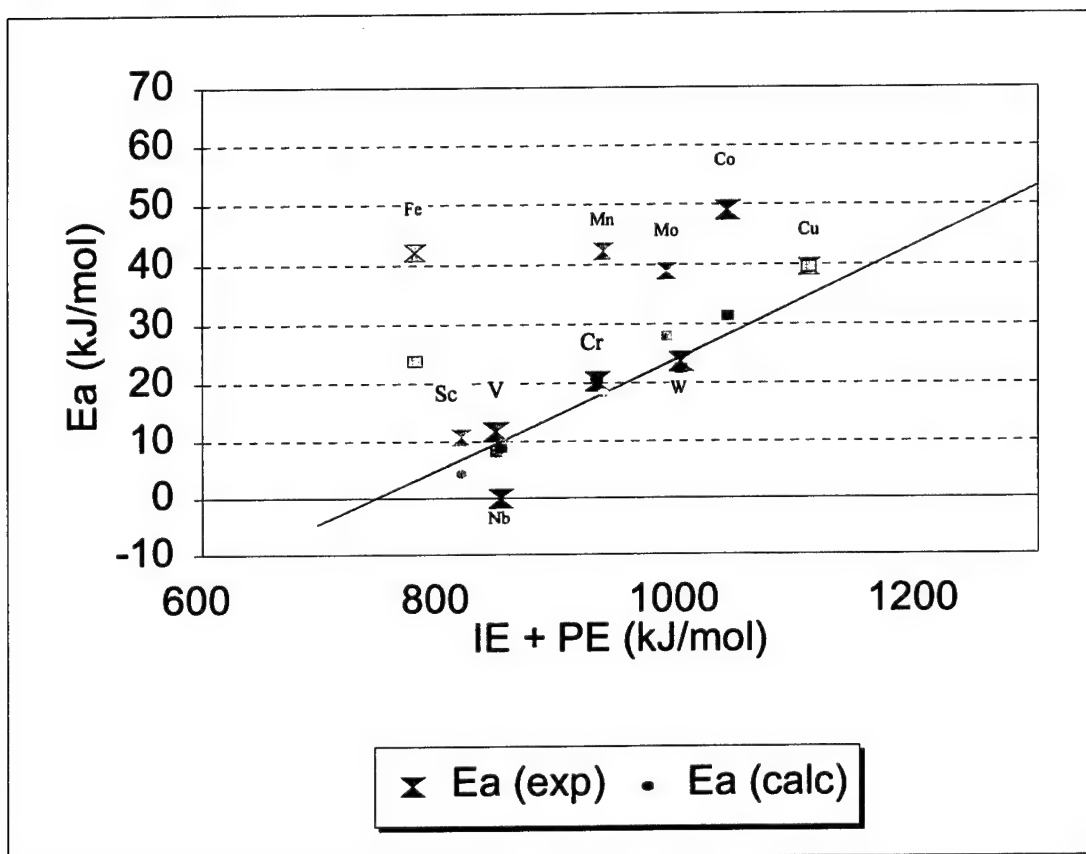
Temperature (K)	Sc ($a^2D_{3/2}$)	V ($a^4F_{3/2}$)	Cr (a^7S_3)	Co ($a^4F_{9/2}$)	Ni (a^3F_4, a^3D_3)
298	1.4E-12	6.0E-13	1.1E-14		1.8E-13
323		8.3E-13			
333		9.0E-13	3.0E-14		
348	2.7E-12	1.1E-12	3.6E-14		
373	3.6E-12	1.5E-12	6.0E-14		1.7E-13
398	4.3E-12	1.8E-12	8.5E-14		2.4E-13
423	5.8E-12	2.2E-12	1.2E-13		2.4E-13
448	6.8E-12	2.8E-12	1.7E-13	3.7E-16	2.9E-13
473	8.0E-12	2.9E-12	2.3E-13	7.6E-16	3.1E-13
498	9.1E-12	3.3E-12	3.1E-13	1.4E-15	3.2E-13
523	1.1E-11	4.0E-12	4.1E-13	2.5E-15	3.9E-15
548		4.1E-12		4.1E-15	4.4E-13
573		5.0E-12		7.4E-15	6.0E-13
598					6.1E-13
623					7.3E-13
E_a (kJ/mole)					
experimental	11.7±0.2	10.7±0.2	20.4±0.2	49.1±0.2	
calculated	4.5	8.1	20.8	31.5	
A ($/10^{-11}$ cm^{3}s^{-1})	16.0±0.2	4.6±0.3	4.2±0.3	20.0±0.3	

Table 2. Comparison of ground state and electron configuration, calculated and experimental activation energies, the percent difference between the calculated and experimental E_a's, sum of ionization potential and s–p promotion energy, s–d promotion energy, and enthalpies of reaction.

TM	Ground State	Electron Configuration	E_a(exp) kJ/mol	E_a(calc)[5] kJ/mol	% Difference	IE + PE(sp)[5] kJ/mol	PE(sd)[17] kJ/mol	ΔH[7] kJ/mol
Cu	$^2S_{1/2}$	$3d^{10}4s^1$	39.6[10]	39.6	0.0	1110	0	-118
W	$^5D_0$	$5d^46s^2$	23.8[14]	22.6	0.9	1002	35	-508
Cr	$^7S_3$	$3d^54s^1$	20.4	20.8	1.9	932	0	-291
Os	$^5D_4$	$5d^66s^2$	38.1[19]	34.5	10.4	1124	62	-388
Ta	$^4F_{3/2}$	$5d^36s^2$	13.6[20]	17.5	22.2	969	117	-672
Ni	$^3F_4$	$3d^84s^2$	α	32.7	—	1045	2	-206
Mo	$^7S_3$	$4d^55s^1$	39.0[11]	28.1	38.8	990	0	-430
V	$^4F_{3/2}$	$3d^34s^2$	10.7	8.1	44.4	847	29	-470
Co	$^4F_{9/2}$	$3d^74s^2$	49.1	31.5	55.9	1041	42	-201
Ti	$^3F_2$	$3d^24s^2$	12.5[8]	8.0	56.2	848	78	-501
Fe	$^5D_4$	$3d^64s^2$	42.2[12]	23.9	76.6	993	83	-246
Nb	$^6D_{1/2}$	$4d^45s^1$	0.0[18]	8.9	100.0	851	0	-616
Mn	$^6S_{5/2}$	$3d^54s^2$	42.3[13]	18.4	129.9	937	204	-190
Sc	$^2D_{3/2}$	$3d^14s^2$	11.7	4.5	137.8	818	138	-505

^{a}Follows non-Arrhenius behavior.

Table 3. Removal rate constants for the excited states of Cr.

State	Second-Order Rate Constant $k_{2nd}/10^{10}$ cm^{3}s^{-1}
a^5S_2	0.95
a^5D_0	1.7
a^5D_1	1.8
a^5D_2	1.8
a^5D_3	1.5
a^5D_4	1.6

Table 4. Rate constants for Ni + N$_2$O as a function of temperature and pressure.

Temperature (K)	State	Total Pressure (Torr)	Second-Order Rate Constant $k_{2nd}/10^{14}$ cm^{3}s^{-1}
298	a^{3}D$_3$	2.5	6.4
		5.0	7.9
		10.0	11.5
		15.0	13.8
		20.0	16.6
		50.0	21.8
		75.0	27.2
		100	29.4
		125	35.4
		150	40.2
		200	49.2
	a^{3}F$_4$	20	16.8
		75	23.7
348	a^{3}D$_3$	2.5	14.3
		10	13.6
		20	17.3
		50	19.4
373		20	16.8
398		20	24.7
	a^{3}F$_4$	20	22.2
423	a^{3}D$_3$	20	24.2
448		20	29.2
		50	28.4
	a^{3}F$_4$	20	31.6
473	a^{3}D$_3$	20	30.6
498		20	31.1
	a^{3}F$_4$	20	32.8
523	a^{3}D$_3$	10	38.6
		20	40.4
		50	41.9
		100	42.6
548		10	46.8
		20	43.9
		50	45.8
573		20	61.6
		50	54.4
	a^{3}F$_4$	20	59.0
598	a^{3}D$_3$	10	72.0
		20	62.2
623		10	72.9

ENDNOTES

[1] Brown, T. L. "The Chemistry of Metallic Elements in the Ionoshpere and Mesosphere," *Chem. Rev.* 1973, 73, 645.

[2] Eden, J. G. *Photochemical Vapor Deposition*; Wiley: New York, 1992.

[3] Morss, Lester R. "Transition Elements," New Grolier Multimedia Encyclopedia, Version 6.03, Grolier Inc., 1993.

[4] Eikind, J. L.; Armentrout, P. B. "State-Specific Reactions of Atomic Transition-Metal Ions with H_2, HD and D_2: Effects of d Orbitals on Chemistry," *J. Phys. Chem.* 1987, 91, 2037.

[5] Futerko, P. M.; Fontijn, A. "Activation barriers for series of exothermic homologous reactions. I. Metal atom reactions with N_2O," *J. Chem Phys.* 1991, 95, 8065-8068.

[6] D. Ritter and J. C. Weisshaar, "Kinetics of Neutral Transition Metal Atoms in the Gas Phase: Oxidation of Sc(a^2D), Ti(a^3F), and V(a^4F) by NO, O_2, and N_2O." *J. Phys. Chem.* 1990, 94, 4907.

[7] M. W. Chase, Jr., C. A. Davies, J. R. Downey, Jr., D. J. Frurip, R. A. McDonald, and A. N. Syverud, eds., JANAF Thermochemical Tables, 3rd ed., *J. Phys. Chem. Ref. Data*, 14 (1985) Suppl. 1.

[8] Campbell, M. L.; McClean, R. E. "Kinetics of Neutral Transition-Metal Atoms in the Gas Phase: Oxidation Reactions of Ti (a^3F) from 300 to 600K," *J. Phys. Chem.* 1993, 97, 7942.

[9] Fontijn, A.; Blue, A. S., A. S. Narayan and P. N. Bajaj, "Gas-Phase Oxidation Kinetics of Toxic Metals at Incinerator Temperatures. The Reactions of Chromium Atoms with HCl, N_2O, Cl_2, and O_2," *Combust. Sci. and Tech.* 1994, 101, 59.

[10] Narayan, A. S.; Futerko, P. M.; Fontijn, A. "A High-Temperature Photochemistry Study of the Reaction between Ground-State Cu Atoms and N_2O from 470 to 1340 K," *J. Phys. Chem.* 1992, 96, 290.

[11] McClean, R.E.; Campbell, M. L.; Goodwin, R. W. "Depletion Kinetics of Mo (a^7S_3, a^5S_2, a^5D_j) by N_2, SO_2, CO_2, N_2O, and NO," *J. Phys. Chem.*, 1996,100, No. 18., 7502.

[12] Campbell, M. L.; Metzger, J. R. "Kinetic Study of the Reaction of Fe (a^5D_J) with N_2O from 398 to 620 K," *Chem. Phys. Lett.*, 1996, 253, 158.

[13] Campbell, M. L. "Kinetic Study of the Reaction of Mn $(a^6S_{5/2})$ with N_2O from 448 to 620 K," *J. Chem. Phys.*, 1996,104,7515.

[14] Harter, J. S. S.; Campbell, M.L., McClean, R.E., "Depletion Kinetics of Low-Lying States of Tungsten in the presence of NO, N_2O, and SO_2," *Int. J. Chem Kinet.* 1997, 29, 367.

[15] Martin, G. A.; Fuhr, J. R.; Wiese, W.L. "Atomic Transition Probabilites Scandium through Manganese," *J. Phys. Chem. Ref. Data*, 1988, 17 Suppl.3.

[16] Plane, J. M. C., " A Kinetic Study of the Reaction Li + N_2O: Non - Arrhenius Behavior Over the Temperature Range 363 -900 K," *J. Phys. Chem.* 1987,91,6552.

[17] C.E. Moore, "Atomic energy levels as derived from the analysis of optical spectra," NSRDS-NBS Circular No. 35 (US GPO, Washington, 1971).

[18] R.E. McClean, M.L. Campbell, E.J. Kölsch, "Depeletion Kinetics of Niobium Atoms in the Gas Phase," *J. Phys. Chem.* 1997, 101, 3348.

[19] M.L. Campbell. "Temperature-Dependent Study of the Kinetics of Os (a^5D_4) with N_2O and O_2." *J. Phys Chem.* 1996, 100, 19430.

[20] M.L. Campbell, K.L. Hooper. "Temperature Dependent Study of the Kinetics of Ta $(a^4F_{3/2})$ with O_2, N_2O, CO_2 and NO." *J. Chem.Soc. Faraday Trans.*, in press.